A STUDY OF THE 21-cm LINE IN THE SOLAR NEIGHBOURHOOD

by

VIRINCHIPURAM R. VENUGOPAL

M.A., University of Madras, 1956

M.A., University of California, 1965

A THESIS SUBMITTED IN PARTIAL FULFILMENT OF
THE REQUIREMENTS FOR THE DEGREE OF
DOCTOR OF PHILOSOPHY

in the Department
of
PHYSICS

We accept this thesis as conforming to the required standard

THE UNIVERSITY OF BRITISH COLUMBIA

May, 1969

Department of Physics

The University of British Columbia
Vancouver 8, Canada

Date May 28, 1969

ABSTRACT

Title of Thesis: A STUDY OF THE 21-cm LINE IN THE SOLAR NEIGHBOURHOOD

Supervisor: DR. W. L. H. SHUTER

A survey of 21-cm line emission at points equally spaced over the entire sky visible from Penticton, British Columbia, has been made, and the profiles obtained at the intermediate galactic latitudes have been used to determine several of the properties of the distribution of the gas in the solar neighbourhood and to study the dynamics of the gas, including the determination of solar motion with respect to gas, the distribution of random velocities and the departures of gas velocities from circular motion.

TABLE OF CONTENTS

LIST OF TABLES

LIST OF FIGURES

ACKNOWLEDGEMENTS

I wish to express my grateful thanks to Dr.W.L.H. Shuter for suggesting to me this investigation and for the guidance and advice provided during the course of this research.

My sincere thanks are due to Dr.J.A. Galt for making available the facilities at the Dominion Radio Astrophysical Observatory , Penticton, to Dr.P.E. Argyle for permitting the use of the 100 channel spectrometer, to Dr.C.H. Costain and Dr.R.S. Roger for assistance with computer programming and helpful discussions.

It is a pleasure to acknowledge the assistance given by all the members of both the technical and office staff of the Observatory.

Financial aid from the University of British Columbia in the form of Graduate Assistantship is also appreciated.

INTRODUCTION

Prediction and discovery of 21-cm line radiation:

The most abundant element in the universe is hydrogen. It is the building material of the stars and galaxies. Yet, until about eighteen years ago astronomers had not succeeded in measuring the neutral hydrogen content of the interstellar medium of our Galaxy. This was because in its unexcited state neutral hydrogen does not emit any radiation in the visible frequency range. But today the 21-cm radio frequency radiation is a very important tool to the astronomer. During a colloquium on the investigations of Jansky (37, 38) and of Reber (56, 57) organised by the Nederlandse Astronomen Club in 1944 Van de Hulst (34) predicted that if a hydrogen atom was in its unexcited or ground state, designated by $1\,^2S_{1/2}$, the magnetic field of the proton and electron could change from parallel to anti-parallel orientations and a spectral line should be emitted at a frequency of 1420 MHz and that there appeared to be a good chance of detecting this transition from the vast but sparsely distributed neutral hydrogen content of the Galaxy. Shklovsky (61) on the basis of the transition probability between hyperfine components of the ground state of hydrogen atom showed that this spectral line should have been detectable in the galactic radio spectrum even with the equipment available at the time. Subsequently the discovery was made in 1951 by Ewen and Purcell (23 (a),(b)) at Harvard University by the detection of the 21-cm line from galactic atomic hydrogen. This detection was confirmed within a few weeks by Muller and Oort (47) in Leiden and by Christiansen and Hindman (53) in Sydney. This discovery was exciting not only because this happened to be the first spectral line to be discovered in solar or cosmic radio waves but also because it opened up a new field of astronomical research - 21-cm line Astronomy - with possibilities of greatly extending our knowledge of the Galaxy and the universe. In fact, since the initial discovery in 1951 hydrogen line investigations have accounted for considerable part of the effort in radio astronomy. The 21-cm line of neutral hydrogen was the only spectral line observed in cosmic radio waves until 1963, when the radio frequency spectrum at a wave length near 18-cm of the OH (hydroxyl) radical in interstellar space was detected by the M.I.T. radio astronomy group using the 84 ft. parabolic antenna of the Millstone Hill Observatory of Lincoln Laboratory (70). Since 1964 many spectral lines - the recombination lines - of excited atomic hydrogen and helium corresponding to transitions involving high principal quantum numbers have been detected in HII regions.

The discovery of this spectral line of atomic hydrogen in the ground state led to numerous studies of galactic structure, physics of the interstellar medium and hydrogen distribution in nearby external galaxies. As a necessary background the current knowledge of the galactic system is briefly reviewed here.

General composition of the Galactic system:

The structure of the Milky way Galaxy (or simply, the Galaxy) is shown in fig. 1, and the space distribution of the principal objects in the Galaxy is schematically illustrated in fig. 2, which represents a meridian cross section of the Galaxy through the sun. It is a vast wheel shaped system of some hundred billion stars with a diameter that probably exceeds 30 Kiloparsecs. The mass of the Galaxy is about 10^{10} $M_{\odot}$. The flattened shape of the Galaxy is a consequence of its rotation. The sun, about 10 Kiloparsecs from the centre out to the rim, moves at a speed of about 250 KMS^{-1} to complete its orbital revolution about the galactic centre in about 200 million years. At the centre of the Galaxy, the nucleus, the stars are somewhat closer together than they are in the solar neighbourhood. Extending outward from the nucleus and winding through the disk of the Galaxy are the spiral arms. The spiral arms consist of vast clouds of gas and cosmic dust - the so called interstellar medium. It is in the interstellar gas and dust clouds of the spiral arms that star formation is believed to be still taking place. The sun is believed to be located in the local arm.

In addition to the individual stars and clouds of inter-stellar matter the Galaxy contains many star clusters. The most common are the 'open' or 'galactic' clusters which are located in the main disk of the Galaxy and are usually in or near spiral arms. Besides the open clusters there are over a hundred globular clusters. These are scattered in a roughly spherical distribution about the Galaxy. They form more or less spherical 'halo' or 'corona' surrounding the main body of the Galaxy. Mrs. Hogg (33) lists positions, descriptions and distances of the 514 galactic clusters and 119 globular clusters.

The interstellar clouds and the O and B type stars, hot super giant stars recently born from them and forming a very thin galactic layer only 1/100 as thick as its diameter, comprise 'extreme population I objects'. In addition to the globular clusters the RR Lyrae stars that are metal poor and extreme subdwarfs have a nearly spherical distribution around the galactic centre. This class is called the 'halo population II'. The motion of the objects belonging to these extreme classes differ in a way corresponding to their difference in distribution. While the objects belonging to population I move in almost circular orbits around the galactic centre the halo population II stars travel in elongated orbits that are often strongly inclined to the galactic plane. Some properties of stellar populations are listed in Table 1.

The youngest stars are those of population I whose distribution and motions still indicate the spiral arms in which they were born. The first reliable determinations of the galactic spiral structure based on the distribution of HII regions emitting the Hα line and also on the distribution of O associations in the neighbourhood of the sun was made by Morgan and his colleagues (45, 46) at the Yerkes Observatory of the University of Chicago. (Fig. 3). It has also been noticed from studies of the distribution of galactic clusters, Cepheid variables and B stars of different ages only the objects younger than about 20 million years are distinctly concentrated in the arms. They are still near their birth places where they condensed from the gas; their older counterparts have had time to wander. This suggests that the spiral arms are fundamentally patterns of gas rather than stars.

It has been recognized that light from the stars is not only reddened and weakened by the interstellar gas and dust during its passage through space, but it is also polarized (31, 32). This polarization suggests that something must be causing alignment of the interstellar grains responsible for the reddening. The galactic magnetic field is an obvious choice. The association of a magnetic field with the Galaxy is also suggested by the phenomenon of galactic cosmic rays, the galactic nonthermal radiation and the maintenance of the galactic spiral arms.

Previous 21-cm line studies and some important results:

With the breakthrough that came in galactic astronomy in 1951 by the discovery of the 21-cm line in emission of neutral hydrogen much valuable information has accumulated in extending our knowledge of the properties of the gas component of the interstellar medium in the solar neighbourhood as well as the overall large scale structure of our Galaxy. These are briefly reviewed in the following paragraphs.

Galactic conditions in the solar neighbourhood:

Basic information on the density of interstellar matter has been obtained from the intensity of the hydrogen emission line at 21-cm. The data obtained by Van de Hulst, Muller and Oort (35) indicate a mean density of 0.7 neutral H-atom/cm^3 in the solar neighbourhood. Since the 21-cm line may be more nearly saturated than has been assumed, and since the ionized H-atoms will increase the mean density slightly, the total mean interstellar gas density is taken as equivalent to 1 H-atom/cm^3, near the galactic plane. This value accounts for only 20% of the mass density in the general vicinity of the sun calculated by Oort (50, 51). About 40% of the density is accounted for by stars of known type. Roughly 40% remains unexplained. The invisible mass may be molecular hydrogen and (or) very faint stars.

The ratio of dust to neutral hydrogen has been shown by Lilley (41) to be roughly constant over large regions but the proportionality fails (8,28), when smaller regions are examined. Recent work by Heiles (27) has shown that OH emission is expected in dust clouds in which 21-cm line emission is not observed. The kinetic temperature of Hl indicated by saturation intensities of the 21-cm line is 125^{o} K which has been pointed out by Kahn (39) to be a harmonic mean temperature weighted by density. Much lower temperatures have been noticed in individual gas clouds . (13,14,55,58,62). The temperature of HII regions is very uncertain at present. The optical methods yield a kinetic temperature of 10,000^{o}K, whereas radio recombination line methods give temperatures around 5000^{o} K.

The observations of the angles of polarization of star light suggest that the lines of magnetic force in the solar neighbourhood are preferentially oriented along a spiral arm (31, 32). The general properties of the gas in the solar neighbourhood have been obtained from observations at 21-cm of neutral hydrogen at intermediate latitudes. The earlier results were from the three extensive surveys (15,21,22,43,44) away from the Milky Way strip. The Carnegie survey of Erickson et al and Sydney surveys of McGee et al showed that hydrogen density is predominantly horizontally stratified, parallel to the galactic plane. Also these surveys have shown that the velocity distribution of hydrogen is associated with differential galactic rotation and that hydrogen is flowing away from the sun at about 6 KmS^{-1} in the directions of the galactic centre and anticentre in low and medium latitudes and is streaming in from above and below.

In considering the velocity field in the neighbourhood of the sun the irregularities in the distribution of interstellar matter are usually described by the random cloud picture with the cloud about 10 Pc in diameter with a density of about 10 atoms/cm^3 and 8 such clouds per Kiloparsec. The distribution of cloud velocities is exponential with a dispersion of 7 KmS^{-1} (1,48,65). Some authors (17,18) suggest abandoning the cloud model and adopting a model of a continuous medium with density fluctuations. Heiles' (26) high resolution observations do not agree with the 'standard cloud model'.

<u>Results pertaining to large scale structure of the Galaxy</u>:

It was mentioned above that Morgan and his associates delineated by optical means the spiral arms in the solar neighbourhood. They could explore only a small fraction of the Galaxy because of the strong interstellar extinction of optical radiation by the dark obscuring matter that exists in the plane of the Milky Way. The observed galactic obscuration is caused by small particles which are believed to be needle shaped. The size of these small particles is very much less than 21-cm, the wave length of radiation emitted by galactic neutral hydrogen, and therefore the particles have negligible blocking power for such radiation. So, this 21-cm line radiation from galactic atomic hydrogen has been utilized to penetrate the far reaches of the Galaxy and indicate the distribution of neutral hydrogen. Since the interstellar medium is closely associated with extreme Population I stars these surveys give a fair representation of the Population I structure of the Galaxy and have confirmed the spiral nature of the Galaxy. The spiral pattern of the Galaxy was successfully mapped in the 21-cm line surveys of the Netherlands and Australia (52). In spite of this advance in the knowledge about our Galaxy that it is a spiral nebula the ideas of the dynamics of the Galaxy need improvement. One of the very confusing facts is that the rotation curves obtained for the northern and southern hemispheres do not agree in detail and the galactic structure map shows an asymmetry between the two halves. In order to reconcile the data of the two hemispheres Kerr (40) investigated the possibility of an outward motion equal to 7 KmS^{-1} of the local standard of rest. Another possibility that was suggested by Kerr on the assumption that the Galaxy is circularly symmetric on a large scale was a general outward motion of the gas away from the galactic centre throughout the Galaxy. The spiral pattern worked out in this basis becomes more symmetrical. But other studies have not generally supported the idea of the motion of the local standard of rest. Braes (10) tried to find the expansion motion suggested by Kerr, but reached a negative conclusion, and he concluded that his data provided neither proof nor a denial of the expansion law proposed by Kerr. The investigation of Weaver (69) points out that there are localized and rather peculiar radial motions, but they are distributed in a haphazard and clumsy way over the galactic plane. An investigation by Venugopal and Shuter (67) of the solar motion with respect to hydrogen has shown that in the solar neighbourhood there is no systematic relative motion between stars and gas. Thus it is clear that the deviation between the rotation curves for the northern and southern sides is due to large scale deviations from circular motion and that a smoothly varying circular orbit model of galactic rotation can no longer be used, and that the over-all picture of gas distribution and motions is a complex one.

Other interesting facts that have come out of the 21-cm line studies are the 3 Kpc expanding arm, the high velocity clouds in the intermediate latitudes and the clouds at great distances from the plane which suggest streams of gas flowing toward us from a direction of about 130^{o} galactic longitude. 21-cm line studies provide information on the magnetic field of the Galaxy. The possibility of using the 21-cm hyperfine structure for measuring the very weak interstellar magnetic fields by utilising the Zeeman Effect was suggested by Bolton and Wild (9). The results were not conclusive until very recently when Verschuur (68) made a successful attempt at the National Radio Astronomy Observatory and found the existence of a field of 20 micro gauss in a cloud in the Perseus arm and of the order of one microgauss for a cloud in Orion arm. Smith (64) from Faraday rotation measurements of Pulsar CP0950 deduced very small fields in its direction.

It should also be mentioned that 21-cm line research has been applied for studying hydrogen distribution in external galaxies, for the determination of distances to radio sources including quasars and pulsars and for the measurement of the density of the intergalactic medium.

PHYSICS OF THE 21-Cm. LINE

Origin of the line:

In a relatively narrow frequency interval centred about 1420.4 MHz. ($\lambda = 21$ cm.) the intensity of the radio frequency radiation received from a typical region of the Galaxy is double that of adjacent portions of the spectrum. This is due to the inherent properties of the hydrogen atom. The details of the origin of this 1420.4 MHz radiation and other galactic radio frequency lines are reviewed by Barrett (3). A brief description of the formation of the neutral hydrogen spectral line is given below.

In atomic and molecular systems the electrons and nuclei can take up only those motions and orientations that yield a discrete set of internal energies - the energy levels. In a bound system the energy is 'quantized". Similarly, the various angular momenta associated with the electrons, nucleus or both are quantized.

The angular momenta necessary to specify the energy states of an atom are: 1) the total electronic orbital angular momentum $\vec{L}$, 2) the total electronic spin momentum $\vec{S}$, 3) the total electronic angular momentum $\vec{J} = \vec{L} + \vec{S}$, 4) the nuclear spin momentum $\vec{I}$, and 5) the total atomic angular momentum $\vec{F} = \vec{I} + \vec{J}$. From quantum mechanics it is known that the total orbital angular momentum $\vec{L}$ is given by an expression involving only the azimuthal quantum number l, viz: $\sqrt{l(l+1)}\,\hbar$. The resultant of the addition of two angular momentum vectors may assume one of several possible values. Thus for a given value of L and S the possible values of J are $L+S$, $L+S-1$, $L+S-2$, ... $|L-S|$. In a similar manner the possible values of F can be obtained.

Energy levels in atoms arise from electric and magnetic interactions of the atomic electrons amongst themselves and with the nucleus. The most important of these interactions from the standpoint of Radio Astronomy is that between the magnetic moment of the electron and the magnetic moment of the nucleus, that is "the hyperfine energy". The electron, because of its inherent properties and because of its motion about the nucleus, produces a magnetic field at the nucleus. This creates different energies of the system for various orientations of the nuclear magnetic moment with respect to this field. This interaction always occurs in atomic system when neither the nuclear angular momentum $\vec{I}$ nor the total electronic angular momentum $\vec{J}$ is zero. If the internal energy of the atom without inclusion of hyperfine effects is E_o, the total internal energy becomes

$$E = E_o + E_M = E_o - \vec{\mu}_I \cdot \vec{H}_J \qquad \text{---------- } 1$$

where the magnetic interaction energy E_M is the negative of the vector dot product of the nuclear magnetic moment $\vec{\mu}_I$ and the magnetic field due to the electron $\vec{H}_J$. For a hydrogen-like atom the hyperfine magnetic interaction energy can be expressed in terms of the quantum numbers F,I,J and L and the physical constants by (5,6):

$$E_M = g_I\left(\frac{m}{M}\right)\frac{\alpha^2 hcRZ^3}{n^3}\left[\frac{F(F+1)-I(I+1)-J(J+1)}{J(J+1)(2L+1)}\right] \quad \text{-----} 2$$

where g_I is the nuclear 'g' factor which is characteristic of a particular nucleus and may be positive or negative,

m mass of electron

M mass of nucleus

α fine structure constant $= \frac{2\pi e^2}{hc} = 7.2973 \times 10^{-3}$

R Rydberg constant $= \frac{2\pi^2 m e^4}{c h^3} = 1.09737 \times 10^5 cm^{-1}$

Z ionic charge

and n the effective quantum number of the hydrogen-like level.

This equation represents the energy of interaction between the magnetic field of the electron and the nuclear magnetic moment. When the nuclear spin momentum is zero corresponding to $\vec{\mu}_I = g_I \mu_N \vec{I} = 0$, $F = J$ and E_M goes to zero. However, for a given I and J not zero, various values of F are possible corresponding to different orientations of $\vec{J}$ relative to $\vec{I}$ and the equation yields different values of the energy for the different orientations.

The transition frequency ν of radiation emitted (or absorbed) is given by the well known Bohr condition:

$$\nu = \frac{E_f - E_i}{h} \quad \text{-----} 3$$

where E_f and E_i are the energies of the final and initial states of the atom respectively. This equation allows the prediction of the transition frequencies if the energies of the states and selection rules are known. The atomic hyperfine energies of hydrogen are given by equation 2 above and the selection rule for hyperfine transitions is $\Delta F = \pm 1, 0$ with jumps $F=0$ to $F=0$ forbidden. The $1 \rightarrow 0$ transition is then equivalent to a spin flip.

The frequency of the transition from a state $F+1$ to a state F is given by

$$\nu = 2\, g_I \left(\frac{m}{M}\right) \frac{\alpha^2 c R Z^3}{n^3} \cdot \frac{F+1}{J(J+1)(2L+1)} \quad \text{-----4}$$

From this expression the transition frequency for the hydrogen hyperfine levels can be predicted.

It is well known that the ground state of hydrogen $1\,^2S_{1/2}$, splits into two very close levels on account of its hyperfine structure, due to the mutual interaction between the intrinsic magnetic moments of the proton and the electron (72). The $1\,^2S_{1/2}$ state of atomic hydrogen is characterized by $n=1$, $L=0$, $S=\frac{1}{2}$ and $J=\frac{1}{2}$. The possible values of F are 1 and 0. This transition called 'a 'spin flip' results in the electron spin flipping from a position parallel to the nuclear spin in the $F=1$ level to an anti-parallel position in the $F=0$ level. The transition occurs between states having the same L quantum number i.e., $L=0$ and is therefore a magnetic dipole transition. The latest value for the frequency of the transition in free space, at zero magnetic field and zero absolute temperature is 1420,405, 751.7860 ± 0.0046HZ. (4).

Transition probability:

The probability for a spontaneous $1 \rightarrow 0$ transition is given by the Einstein A Coefficient:

$$A_{10} = \frac{64\pi^4\beta^2}{3h\lambda^3} = 2.85\times10^{-15}\,\mathrm{sec}^{-1} \text{ - - - - - } 5$$

where β is the Bohr magneton $= \frac{eh}{4\pi mc} = 0.92732\times10^{-20}$ erg gauss^{-1}. The mean life time of the 'excited' hydrogen (i.e. of the hydrogen in state $F=1$) is $\tau_{10}=\frac{1}{A_{10}}=3.5\times10^{14}$ sec. or 11 million years. The reasons for such a long life time are the low frequency of the line (since $A_{nn'}\propto\nu^3$) and the fact that it comes from a forbidden transition (transition probabilities for magnetic dipole radiation are of the order of 10^5 times as small as those for electric dipole radiation regardless of frequency). The natural half width of this line has the minute value 5×10^{-16} Hz . In the interstellar medium the basic elementary processes determining the population of the hyperfine levels are collisions of the first and second kinds. In collisions of the first kind a change of Kinetic energy of translation into excitation energy takes place by collision. Collisions of the second kind include not only the exact reverse of collisions of the first kind but also all other processes in which an atom or molecule gives up excitation energy by colliding with another partner. In equilibrium the number of collisions of the first kind per unit volume and time equals the number of collisions of the second kind. Then the population of the two hyperfine levels 1 and 0 will be given by Boltzmann's formula:

$$\frac{n_1}{n_0} = \frac{g_1}{g_0}\, e^{-h\nu/kT_S} \text{ - - - - - } 6$$

where g_1 and g_0 are the statistical weights of the sublevels given by $g=2F+1$ and T_S is known as the 'spin temperature'. It should not be simply assumed that the spin temperature T_S is equal to the kinetic temperature T_K of the atoms. Purcell and Field (54) and Field (24) made a careful analysis of the various processes which are competing to establish the relative populations of the energy levels for the hydrogen line from interstellar space and found that collisions are the dominant factor in controlling the spin states and therefore the spin temperature is effectively equal to the Kinetic temperature.

Equation 6 can be rewritten as $\frac{n_1}{n_0} = 3 \cdot e^{-\frac{h\nu_{10}}{kT_K}}$. Further because the energy difference between the two sublevels is so small $\frac{h\nu_{10}}{k}$ is small (0.0681 K) and the exponential above is close to unity for all reasonable values of T_K. Therefore, $\frac{n_1}{n_0} \doteq 3$. Since the initial state of the transition giving rise to the 21-cm. line is maintained in equilibrium by collisions the energy emitted in this line depends on the internal energy of the interstellar gas which means that the monochromatic galactic radio emission is thermal.

Although the Einstein A coefficient is very small for this transition and most of the transitions from the upper to the lower state are radiation-less as a result of collisions of the second kind, yet because of the vast number of hydrogen atoms in the galactic disk the hydrogen line from the interstellar medium could be detected.

<u>The formation of Emission and Absorption lines</u>:

Equation of Transfer for the 21-cm. line:

Let us first consider the transfer of radiation along any line of sight passing through some assembly of atoms. Let the volume coefficients of absorption and emission in the frequency element $(\nu, \nu + d\nu)$ at the point in the line of sight at distance S from the observer be K (ν) and J $(\nu)\,d\nu$ respectively. Then the specific intensity, I $(\nu)\,d\nu$, of the radiation at any point is given by the equation of transfer:

$$\frac{dI(\nu)}{ds} = J(\nu) - k(\nu)I(\nu) \quad ----- 7$$

The solution to this can be obtained from an elementary analysis. Since the intensity at any point S and a given direction results from the emission at all points beyond S, reduced by the factor $e^{-\int_0^s k(\nu)ds'}$ to allow for the absorption by the intervening matter we can write

$$I(\nu) = \int_0^\infty J(\nu)\, e^{-\int_0^s k(\nu)\,ds'}\, ds \quad ----- 8$$

for the intensity of the emergent radiation. The observed intensity is usually expressed in terms of the brightness temperature $T_b(\nu)$ which is given by the Rayleigh-Jeans formula:

$$T_b(\nu) = \frac{I(\nu)c^2}{2k\nu^2} \quad ----- 9$$

Here 'k' is the Boltzmann's constant.

The ratio of the emission and absorption coefficients can be written as follows by the Planck-Kirchhoff's law:

$$\frac{J(\nu)}{K(\nu)} = \frac{2\nu^2}{c^2}kT \quad (\text{or})\; J(\nu) = \frac{2\nu^2}{c^2}kT.K(\nu) \quad ----- 10$$

where T refers to the spin temperature which is equal to the kinetic temperature here.

Therefore, we obtain

$$T_b(\nu) = \int_0^\infty T\,K(\nu)\exp\left[\int_0^s K(\nu)\,ds'\right]ds = \int_0^{\tau'(\nu)} T e^{-\tau(\nu)}\,d\tau(\nu) \quad ----- 11$$

where $\tau(\nu) = \int_0^s K(\nu)ds'$ is the optical depth and $\tau'(\nu)$ is the optical depth of the whole Galaxy in a given direction. If the kinetic temperature of the whole Galaxy is constant, then

$$T_b(\nu) = T(1-e^{-\tau'(\nu)}) \text{-----} 12$$

This is the general relation for an emission line.

The presence of continuous spectrum:

Absorption line formation:

This means that we should introduce the continuous absorption and emission coefficients $K_1(\nu)$ and $J_1(\nu)$ for the continuum. Now the equation of transfer becomes:

$$\frac{dI(\nu)}{ds} = J(\nu) + J_1(\nu) - [K(\nu)+K_1(\nu)]I(\nu) \text{----} 13$$

As before we get:

$$T_b = \frac{c^2}{2k\nu^2}\int_0^\infty [J(\nu)+J_1(\nu)] \exp\left\{-\int_0^s [K(\nu)+K_1(\nu)] ds'\right\} ds \text{---} 14$$

and for the region in the continuum adjacent to the radio line, where $J(\nu)$ and $K(\nu)$ are equal to zero,

$$T_b = \frac{c^2}{2k\nu^2}\int_0^\infty J_1(\nu) \exp\left[-\int_0^s K_1(\nu) ds'\right] ds \text{----} 15$$

The galaxy can be considered transparent for decimetre radio waves in the continuum; so, equation 15 becomes

$$T_b = \frac{c^2}{2k\nu^2}\int_0^\infty J_1(\nu)\, ds \text{-----} 16$$

Also, in the region of the 21-cm. line $K(\nu) \gg K_1(\nu)$.

So equation 14 can be written as:

$$T_b(\nu) = \frac{c^2}{2k\nu^2}\int_0^\infty [J(\nu)+J_1(\nu)] e^{-\tau(\nu)} ds$$
$$= \frac{c^2}{2k\nu^2}\int_0^\infty J(\nu) e^{-\tau(\nu)} ds + \frac{c^2}{2k\nu^2}\int_0^\infty J_1(\nu) e^{-\tau(\nu)} ds \text{----} 17$$

Using equations 12 and 16 in 17 we have

$$T_b(\nu) = T\left[1-\exp(-\tau'(\nu))\right] + T_b \langle \exp(-\tau(\nu)) \rangle \text{---} 18$$

The difference in brightness temperature between different points on the line profile and the continuum will be equal to:

$$\Delta T = T\left[1-\exp(-\tau'(\nu))\right] - T_b\left[1-\langle \exp(-\tau(\nu))\rangle\right] \quad ---19$$
$$= \left[T-T_b\right]\left[1-\langle \exp(-\tau(\nu))\rangle\right] \text{ taking } \tau'(\nu) \text{ and } \tau(\nu)$$

to be of the same order.

It is evident from the above that the relative size of T and T_b determine whether there will result an emission line, no line or an absorption line.

If hydrogen absorption is observed by directing the antenna to a continuum source of small angular diameter:

$$T_b(\nu) = T(1-e^{-\tau(\nu)}) + T_b \frac{\Omega_S}{\Omega_B} e^{-\tau_S(\nu)} \quad -----20$$

where $\tau(\nu)$ is the effective opacity spread over Ω_B, the beam angle and $\tau_S(\nu)$ that part confined to Ω_S, the source solid angle.

$$T_A = T_B \frac{\Omega_S}{\Omega_B} \quad -----21$$

The observed profile is given by

$$\Delta T'(\nu) = \overline{\Delta T(\nu)} - T_A\left(1-e^{-\tau_S(\nu)}\right) \quad -----22$$

where $\overline{\Delta T(\nu)} = T(1-e^{-\tau(\nu)})$ is the expected profile. From the observables $\overline{\Delta T(\nu)}$, $\Delta T'(\nu)$ and T_A we can get $\tau_S(\nu)$ which is of very great astronomical interest.

Absorption measurements provide a technique for studying individual hydrogen clouds, for the angular diameter of the radio stars is typically a few minutes of arc so that only a narrow pencil of rays joins the source to the earth, and the few clouds through which this pencil cuts can usually be seperated in depth by their differing Doppler shifts.

EQUIPMENT AND OBSERVATIONS

A survey of neutral hydrogen of the whole sky visible from Penticton has been undertaken in order to obtain a catalogue of profiles spaced 5° arc apart in the sky with the points surveyed given in the new system of galactic co-ordinates. On the completion of the survey part of the collected data was used to determine several of the properties of the nearby gas, to describe the spatial distribution of random velocities of neutral hydrogen in the solar neighbourhood for which there was no previous information. This project forms the subject of Chapter IV. Also, an analysis of the departures of the velocities of nearby gas from circular motion is presented in chapter V. In the present chapter a brief description of the equipment used and the observations made is given.

The observations described here were obtained in August and September 1967, using the 25.6 metre paraboloid and the 21-cm. line facilities (42) of the Dominion Radio Astrophysical Observatory, Penticton (longitude $=$ 119° 37' W, latitude $=$ 49° 19' N) with a new 100 channel filter spectrometer designed and constructed by Dr. P.E.Argyle. The 25.6 metre antenna which has a half power beam width of 36' at $\lambda = 21$-cm. is equatorially mounted, and at its location is far enough south that observations down to declination -30° are possible. Any part of the sky visible at the site can be observed directly, and the telescope position is indicated by synchronous repeaters reading declination, right ascension and hour angle. The telescope can track in hour angle at the sidereal rate. The radio frequency preamplifier is an electron beam parametric amplifier (Adler tube) similar to the one described by Adler, Hrbek and Wade (2), and is operated in the nondegenerate mode for hydrogen-line studies with the spectrometer.

The hundred channel radio frequency spectrometer is built around a commercially produced "contiguous comb filter". This filter system contains 100 crystal filters, each of 10 KHz. band width. The band edges of adjacent filters coincide, so that the total band width of the system is 1 MHz. The filters are so designed that the frequency components of signal not passed by a filter are reflected so that they are available as input signal to other filters; in other words, the filters do not act as short circuits to frequencies they do not transmit. All amplification is made in front of the contiguous filter, thus avoiding the problem of maintaining uniform gain in one hundred independent amplifiers. The centre frequency of the spectrometer is 10.7 MHz., the last intermediate frequency of the hydrogen receiver. The standard integration time used in the spectrometer is 60 seconds. Two banks of integrating capacitors are used so that one bank can be used while the other is being charged. Thus no observing time is lost during read out . Read out of a bank of capacitors is done with a 'binary read out tree' of reed switches. The resultant voltages are read by a digital voltmeter which then commands the card punch to record the 3 digit number just produced. These data are punched on four IBM cards, with the first columns of each card being used for serial number or some identification. The over-all system noise temperature was about 250° K.

The profiles were obtained at positions 5° arc apart along circles of latitude at intervals of 5° . The longitude interval corresponding to the length $\Delta S (= 5^{\circ})$ of a circle of latitude was calculated from the relation $\Delta \ell = \frac{\Delta S}{\cos b}$ and rounded off to the nearest degree. The longitude (l) and latitude (b) are expressed in the new standard system of galactic co-ordinates. (7). In all, over 1200 profiles were obtained, covering the entire sky visible from Penticton. The catalogue of profiles is being prepared for publication. The brightness temperature calibration for the profiles was obtained from repeated observations of the Berkeley calibration profile at $\ell = 207^{\circ}$, $b = -15^{\circ}$ for which the peak intensity was taken as 62° K.

The velocities of hydrogen gas were referred to the local standard of rest (l.s.r.) which required that the observed radial velocities be corrected for Doppler shifts produced by the earth's orbital motion and for the motion of the sun with respect to the mean velocity of Hydrogen in the vicinity of the sun. It has been shown (67) that in the vicinity of the sun there is no appreciable differential motion between the neutral hydrogen and the stars; so in the reduction of the observed velocities to l.s.r. in this survey the standard solar motion (19) defined by $S_{\odot} = 20.0$ KmS^{-1}, $L_{\odot} = 56^{\circ}.2$, $B_{\odot} = +23.2^{\circ}$, $K = 0.0$ KmS^{-1} was used. In the correction for the orbital motion of the earth the eccentricity (e), the mean longitude of perigee (Γ), the obliquity of the ecliptic (ϵ) and the mean longitude of the sun (L) are involved, and these are calculated using the expressions given in the Explanatory Supplement to the Ephemeris (1961).

The profiles of brightness temperature versus radial velocity were automatically plotted at the University of British Columbia computer centre. The co-ordinates to which each profile refers were indicated in the top right hand corner.

The data from the profiles of the intermediate latitude zones were used for the following studies of hydrogen in the solar vicinity:

i) Kinetic temperature; ii) distribution of random motions and iii) departures of velocities from circular motion. These are described in the next two chapters.

ANALYSIS AND INTERPRETATION

This project was undertaken with the principal objective of being able to describe the spatial distribution of random velocities of neutral hydrogen in the solar neighbourhood, for which there was no previous information .

It soon became clear that the main prerequisites for this study were a determination of the solar motion with respect to neutral hydrogen and the requirement that the distribution of hydrogen in the solar neighbourhood obey a simple model, so that a mean distance and hence radial velocity could be assigned for the hydrogen emission of each of our observed profiles.

The solar motion with respect to neutral hydrogen was found to be sufficiently close to the standard solar motion (67) that the standard value could be used. This determination of solar motion with respect to neutral hydrogen was undertaken earlier, and the procedure adopted is described briefly here.

Solar Motion from 21-cm. line Observations:

Radial velocities determined from 21-cm. profiles are normally specified, with respect to the local standard of rest (12), a reference frame travelling with the mean velocity of the stars in the vicinity of the sun. This is achieved by correcting the observed radial velocities for the earth's orbital motion, and for the standard solar motion(19)- the velocity of the sun with respect to the local standard of rest. Because in the 21-cm. line studies of local hydrogen in the Galaxy one would normally wish to specify the radial velocity of galactic hydrogen with respect to the mean velocity of HYDROGEN in the vicinity of the sun, one must recognize the assumption implicit in the above procedure (73) that there is no systematic differential motion between the nearby hydrogen and stars. In our investigations we have in effect measured the differential motion between the nearby hydrogen and stars by measuring the velocity of the sun with respect to the nearby hydrogen. The technique used is similar in principle to the method commonly used in optical astronomy for determination of the solar motion from stellar radial velocities, but a modification is required because in the 21-cm. line case the distance of the observed hydrogen is not usually known.

The observed radial velocity of nearby hydrogen gas with respect to the sun V_r may be represented by the familiar equation (66a)

$$V_r = K - S_\odot \cos B_\odot \cos b \cos (l - L_\odot) - S_\odot \sin B_\odot \sin b + A r \cos^2 b \sin 2l \quad \text{-----} \quad 23$$

where 'K' is a constant term, $S_\odot$ is the speed of the sun with respect to the mean velicity of hydrogen, $L_\odot$, $B_\odot$ are the galactic co-ordinates of the apex of solar motion, r, l, b are the heliocentric co-ordinates of the observed hydrogen gas; and A the Oort constant for radial velocity. The last term in the above equation, $A r \cos^2 b \sin 2l$, represents the contribution to radial velocity resulting from differential galactic rotation on the simple hypothesis of circular motion about the galactic axis, this motion being independent of the vertical distance of the observed gas from the galactic plane. Since 'r' the distance to the gas observed is not well known, the observations were restricted to longitudes 0°, 90°, 180° and 270°, for which $\sin 2l = 0$, and hence the term $A r \cos^2 b \sin 2l$ vanishes. Further, since the above equation is only valid for 'r' small compared to the distance from the sun to the galactic centre, the observations were confined to intermediate latitudes where, due to the thinness of the galactic disk the condition is fulfilled.

Two independent profiles at each of the following 22 positions were obtained and used in the analysis.

Co-ordinates of the profiles used in the analysis

l	b
0°	$+20^\circ$, $+25^\circ$, $+30^\circ$, $+35^\circ$, $+40^\circ$, $+45^\circ$.
90°	-20°, -25°, -30°, -35°, -40°, -45°.
180°	-20°, -25°, -30°, -35°, -40°, -45°.
270°	$+30^\circ$, $+35^\circ$, $+40^\circ$, $+45^\circ$.

Radial velocity $\overline{V}$ averaged over brightness temperature for each profile defined as

$$\overline{V} = \int_{V_1}^{V_2} V\, T_b(V)\, dV \Big/ \int_{V_1}^{V_2} T_b(V)\, dV \quad \text{----- } 24$$

with the limits of integration V_1 and V_2 taken as the velocity values at which the 21-cm. brightness temperature T_b (V) was 10% of its maximum value, was determined with an accuracy of $\pm$ 0.3 KmS^{-1}. These velocities were referred to the sun using tables (30), and the resulting radial velocities, V_r were used to obtain the elements of solar motion $S_\odot$, $L_\odot$, $B_\odot$, and K by means of a least squares solution of the equation

$$V_r = K - S_\odot \cos B_\odot \cos b \cos(l - L_\odot) - S_\odot \sin B_\odot \sin b \quad \text{----- } 25$$

The elements of solar motion relative to neutral hydrogen obtained in this investigation, with their probable errors, are

$$S_{\odot} = 21.1 \pm 1.3 \text{ Kms}^{-1}$$
$$L_{\odot} = 49^{\circ}.2 \pm 8^{\circ}.9$$
$$B_{\odot} = 24^{\circ}.7 \pm 13^{\circ}.7$$
$$K = -0.8 \pm 0.7 \text{ Kms}^{-1}$$

There is no significant difference between our results and the standard solar motion given below for comparison:

$$S_{\odot} = 20.0 \text{ Kms}^{-1}$$
$$L_{\odot} = 56^{\circ}.2$$
$$B_{\odot} = 23^{\circ}.2$$
$$K = 0.0 \text{ Kms}^{-1}$$

Thus our results indicate that in the vicinity of the sun there is no appreciable differential motion between the neutral hydrogen and the stars, and also that no significant errors are introduced in 21-cm. line work by using the standard solar motion to correct observed radial velocities to the local standard of rest.

Besides the determination of the solar motion with respect to neutral hydrogen we require for our analysis of random motions that the hydrogen distribution in the solar vicinity be capable of being described reasonably well by a simple model. McGee and Murray (43) concluded from their low resolution sky survey of neutral hydrogen that the local distribution is substantially horizontally stratified in density, with a number of concentrations of gas embedded in it. We, therefore, tentatively adopt the model that the hydrogen density is a function only of Z , the distance from the sun in a direction perpendicular to the central plane of the galactic disk. This model can be tested in a simple way. Referring to figure 4, we suppose that two planes P and P′ parallel to the central plane of the Galaxy G, and distances Z_o and Z_o' respectively from S, the position of the sun, pass through points at which the average hydrogen density is half that in the vicinity of the sun. If the gas is horizontally stratified in density as required and we assume Z_o corresponds to an optical depth τ_o and 'r' ($= Z_o$ cosec b) corresponds to an optical depth τ , then the model requires $\tau = \tau_o$ cosec b. To allow for the presence of 21-cm. line emission from the galactic halo (or for the inadequacy of the simple picture of the Galaxy adopted) we may include a constant term τ_H and write

$$\tau = \tau_o \operatorname{Cosec} b + \tau_H \quad \text{-----} 26$$

The relation between the brightness temperature T_b observed along the line of sight at latitude b and the kinetic temperature T_K and the optical depth τ of the gas is obtained as follows:

Adding all the elementary contributions along a ray, the brightness temperature in the direction of any ray is given by

$$T_b = \int_{-\infty}^{+\infty} e^{-\tau'} T_K \, d\tau' \quad \text{------} 27$$

where τ' is the optical depth to each element. For a thick layer of isothermal homogeneous gas of temperature T_k and optical thickness τ

$$T_b = \int_0^{\tau} e^{-\tau'} T_K \, d\tau'$$
$$= T_K (1 - e^{-\tau}) \quad \text{------} 28$$

From the above equation we obtain

$$\tau = \ln T_K / (T_K - T_b) \quad \text{-----} 29$$

$$(\text{But} \quad \tau = \tau_o \operatorname{Cosec} b + \tau_H \text{ from } 26)$$

Therefore from (26) and (29)

$$\tau = \ln T_K/(T_K - T_b) = \tau_o \operatorname{cosec} b + \tau_H \text{ -----30}$$

Therefore, if the gas density is horizontally stratified and if the correct choice of T_k is made, a plot of τ vs cosec b based on the observed b and T_b is expected to be a straight line. The effect of an incorrect choice of T_k can easily be predicted. If T_k is chosen too high the plot would curve down at low latitudes where the optical depth becomes appreciable; similarly, if T_k were too low the plot would curve upward at low galactic latitudes.

In this analysis the peak brightness temperature of each profile in the latitude range $+10^\circ$ to $+40^\circ$ was obtained and the mean brightness temperature around each circle of galactic latitude was determined so that variations with galactic longitude were averaged over. Using these mean values of T_b, values of τ were calculated for assumed values of T_k of 80° K, 100° K, 120° K, and 140° K, and graphs of τ vs cosec b were plotted for the northern and southern galactic hemispheres separately. These plots are shown in Figures 5 and 6.

It is seen that a linear relationship is obtained for a kinetic temperature of 120° K. A least squares solution for the best fitting straight line was then made for various temperatures around 120° K, i.e., for 110°, 120°, 130°, and 140° K, and the corresponding values of τ_o and τ_H were found. That combination of T_k, τ_o and τ_H which gave the minimum residual $\sum v^2$:

$$\sum v^2 = \sum_{i=1}^{n} \left[T_{bi} - T_K \left(1 - e^{-(\tau_o \operatorname{cosec} b + \tau_H)}\right) \right]^2 \text{ -----31}$$

(where n is the number of T_b values considered in each plot) was taken as the best representative values of T_k, τ_o and τ_H .

Results and Discussion:

The following values were obtained:

Northern galactic hemisphere $T_k = 120^\circ K$, $\tau_o = 0.07$, $\tau_H = -0.05$.

Southern galactic hemisphere $T_k = 120^\circ K$, $\tau_o = 0.08$, $\tau_H = -0.01$.

Mean values with their estimated errors are:

$$T_k = 120^\circ \pm 15^\circ\ K$$
$$\tau_o = 0.08 \pm 0.01$$
$$\tau_H = -0.03 \pm 0.01$$

The value of $T_k = 120^\circ$ K obtained in this study is in agreement with the usually adopted Leiden value (71).

The optical depth from the sun to the half density points of the galactic disk is $\tau_o = 0.08$, and this value is considered further in the next section.

The negative value for $\tau_H (= -0.03)$ suggests there is no appreciable neutral hydrogen emission from a distribution with spherical symmetry about the sun, and can be accounted for by assuming that the value of τ_o immediately above the sun is slightly less than the average value at points around the sun. This result appears to be in accordance with the general distribution of stars near the sun (20). Since the value of τ_H was derived by averaging over all galactic longitudes, it is not possible from this result to comment on whether neutral hydrogen emission from the galactic halo has been observed, although this could be deduced by further analysis of our basic data.

Distribution of Random Motions

(a) Technique and Analysis

In order to investigate the distribution of random motions in nearby hydrogen gas the axes of the velocity ellipsoid and their directions were determined according to the following procedure.

The brightness temperatures, T_b, of each profile were converted to optical depth values, τ, using $T_k = 120^{\circ}K$ derived above, and the relation $\tau = \ln T_k/(T_k - T_b)$. From the profiles of τ vs radial velocity V, the mean velocity $\bar{V}_{obs}$,

$$\bar{V}_{obs} = \int_{V_1}^{V_2} V\tau(V)\,dV \Big/ \int_{V_1}^{V_2} \tau(V)\,dV \quad ----- 32$$

and the dispersion σ_{total},

$$\sigma_{total} = \left[\int_{V_1}^{V_2} (V - \bar{V}_{obs})^2 \tau(V)\,dV \Big/ \int_{V_1}^{V_2} \tau(V)\,dV \right]^{1/2} ----- 33$$

(with the limits of integration V_1 and V_2 taken as the velocity values at which the 21 cm. brightness temperature $T_b(V)$ was 10% of its maximum value) were calculated for each profile.

Our aim in this study is initially to determine the dispersion in each of the hydrogen profiles attributable to random motion and turbulence σ_r. This can be derived from the relation

$$\sigma_r^2 = \sigma_{total}^2 - (\sigma_{rot}^2 + \sigma_{thermal}^2 + \sigma_{inst}^2) ----- 34$$

where σ_{total} defined in equation (33) is obtained from the profiles, and σ_{rot}, $\sigma_{thermal}$ and σ_{inst} are respectively the dispersion produced by differential galactic rotation, by thermal broadening, and by the instrument pass band.

We consider now the derivation of the latter 3 quantities.

According to the theory of differential galactic rotation the mean radial velocity is given as

$$\bar{V}_{obs} = Ar \sin 2l \cos^2 b + (\bar{V}_p) \quad ----- 35$$

for small heliocentric distances, where r is the mean distance of the emitting hydrogen, A is the Oort constant for radial velocity and $\bar{V}_p$ is the mean value of the peculiar radial velocity. The mean distance is $r = z_o \operatorname{cosec} b$, where z_o is the mean height of the emitting hydrogen from the plane containing the sun. Therefore

$$\bar{V}_{obs} = Az_o \sin 2l \operatorname{cosec} b \cos^2 b \quad ----- 36$$

where the term $\bar{V}_p$ is being disregarded for the mement. Thus from each profile a value of Az_o was obtained, and the mean value $\overline{Az_o}$ from all the profiles was calculated. With this value $\overline{Az_o}$ the theoretical mean velocity that the gas should have in each direction of observation was computed from

$$\bar{V}_{th} = \overline{Az_o} \sin 2l \operatorname{cosec} b \cos^2 b \quad ---- 37$$

Then a linear relationship $\bar{V}_{obs} - \alpha \bar{V}_{th} = v$ was considered, and the value of α found for which $\sum v^2$ was a minimum. It may easily be shown that the constant indicates the nature of the peculiar velocities $\bar{V}_p$. If $\alpha = 1$ the mean of all the values $\bar{V}$ tends to zero. If α deviates from 1 the mean is non-zero, and the value $\overline{Az_o}$ must be corrected to $\alpha \overline{Az_o}$ to allow for the bias so introduced.

To estimate the velocity dispersion produced by differential galactic rotation it is necessary to make an assumption about the manner in which the hydrogen density varies with z.

Two simple models were considered: the first being a uniform density disk, and the second one in which the hydrogen density falls off exponentially with z. The second model was adopted, since it appeared to conform more closely with the profiles. It is easily shown that in the case

$$\tau(V) = \tau(o)\, e^{-V/\bar{V}} \qquad 38$$

where $\bar{V} = \alpha \bar{V}_{th}$ corresponds to the velocity at the scale height z_o. Then the dispersion of each profile due to galactic rotation σ_{rot} for this density distribution was calculated from $\sigma^2_{rot} = \alpha^2 \bar{V}^2_{th}$.

The thermal broadening $\sigma_{thermal}$ was evaluated assuming $T_k = 120^{\circ}K$, and the instrument broadening σ_{inst} was also derived.

The values of σ_r were then used to derive the velocity ellipsoid, a dispersion ellipsoid with three unequal axes, according to the procedure described by Trumpler and Weaver (66b).

First the six second order central moments, μ_{ijk}, of the ellipsoidal distribution were determined by the least squares method from the following equation of condition

$$\begin{aligned}\sigma_r^2(\alpha,\delta) = {} & \gamma_{13}^2\mu_{200} + \gamma_{23}^2\mu_{020} + \gamma_{33}^2\mu_{002} \\ & + 2\gamma_{13}\gamma_{23}\mu_{110} + 2\gamma_{23}\gamma_{33}\mu_{011} \\ & + 2\gamma_{13}\gamma_{33}\mu_{101}\end{aligned} \qquad 39$$

where the direction cosines γ_{13}, γ_{23}, γ_{33} are given by

$$\begin{aligned}\gamma_{13} &= \cos\alpha \cos\delta \\ \gamma_{23} &= \sin\alpha \cos\delta \\ \gamma_{33} &= \sin\delta\end{aligned} \qquad 40$$

From the μ_{ijk} so determined the squares of the semiprincipal axes $(\Sigma_1)^2$, $(\Sigma_2)^2$, $(\Sigma_3)^2$ of the velocity ellipsoid were found as the three roots of the cubic equation in $(\Sigma)^2$:

$$\begin{vmatrix} \mu_{200}-(\Sigma)^2 & \mu_{110} & \mu_{101} \\ \mu_{110} & \mu_{020}-(\Sigma)^2 & \mu_{011} \\ \mu_{101} & \mu_{011} & \mu_{002}-(\Sigma)^2 \end{vmatrix} = 0 \qquad \text{---}41$$

The direction cosines l_1, m_1, n_1 of the axis corresponding to Σ_1, were determined from

$$l_1 = \pm \frac{\Delta_{1,200}}{\sqrt{(\Delta_{1,200})^2+(\Delta_{1,110})^2+(\Delta_{1,101})^2}}$$

$$m_1 = \pm \frac{\Delta_{1,110}}{\sqrt{(\Delta_{1,200})^2+(\Delta_{1,110})^2+(\Delta_{1,101})^2}}$$

$$n_1 = \pm \frac{\Delta_{1,101}}{\sqrt{(\Delta_{1,200})^2+(\Delta_{1,110})^2+(\Delta_{1,101})^2}} \qquad \text{----}42$$

Here

$$\Delta_1 = \begin{vmatrix} \mu_{200} - (\Sigma_1)^2 & \mu_{110} & \mu_{101} \\ \mu_{110} & \mu_{020} - (\Sigma_1)^2 & \mu_{011} \\ \mu_{101} & \mu_{011} & \mu_{002} - (\Sigma_1)^2 \end{vmatrix}$$

and $\Delta_{1, ijk}$ is the cofactor of the term containing μ_{ijk}.

The direction cosines of the axes corresponding to Σ_2 and Σ_3 are obtained by changing the subscript in the above from 1 to 2 and 3.

$\bar{V}_{obs}$ and σ^2_{total} were obtained for a sample of 50 profiles at intermediate galactic latitudes between $\pm 15^\circ$ and $\pm 45^\circ$ and covering 360° in longitude, and the velocity ellipsoid was derived as described above.

(b) <u>Results</u>

The derived mean value of Az_o i.e. $\overline{Az}_o = 2.53$ KmS^{-1}.

The value of α required to minimize the sum of the squares of the residuals $\sum v^2 = \sum(\bar{V}_{obs} - \alpha\bar{V}_{th})^2$ is $\alpha = 0.5$.

From the corrected value $\alpha\overline{Az}_o = 1.26$ KmS^{-1}, and assuming $A \simeq 15$ KmS^{-1} Kpc^{-1} we obtain for the scale thickness of the galaxy in the solar neighbourhood:

$$Z_o = 1.26/15 = 0.084 \text{ kpc.}$$

Therefore the <u>total</u> thickness of the galactic disk measured between points where the hydrogen density is one half that at the position of the sun is $\approx 2\bar{z}_o$ or 168 pc.

In 3 (b) above we obtained $\tau_o =$ 0.08 corresponding to $\bar{z}_o$ so in the solar neighbourhood the optical depth for the 21-cm. can be estimated to be 0.95/kpc.

The axes of the velocity ellipsoid and their directions are:

$$\Sigma_1 = 6.7 \text{ Km s}^{-1} \qquad l = 239^\circ.2 \qquad b = +35^\circ.3$$

$$\Sigma_2 = 4.5 \text{ Km s}^{-1} \qquad l = 160^\circ.3 \qquad b = -14^\circ.9$$

$$\Sigma_3 = 7.8 \text{ Km s}^{-1} \qquad l = 269^\circ.0 \qquad b = -49^\circ.8$$

$$\bar{\Sigma} = \sqrt{1/3[(\Sigma_1)^2 + (\Sigma_2)^2 + (\Sigma_3)^2}$$

$$= 6.5 \text{ Km s}^{-1}$$

$$\text{Mean Error } e(\bar{\Sigma}) = \pm 0.3 \text{ Km s}^{-1}$$

$$\Sigma_1/\Sigma_2 = 1.51$$

Discussion

From this analysis the mean dispersion is equal to 6.5 KmS^{-1} which is in good agreement with other determinations.

The dynamical theory of the stellar system in a steady state developed by Lindblad and Oort (63) shows that the direction of the longer axis of the velocity ellipsoid in the galactic plane (i.e. the vertex) should coincide with the anticentre - centre line, i.e. $\ell = 180^\circ$ and 0°. The direction of this axis corresponding to Σ_1 in the present analysis of this axis is towards $\ell = 239^\circ.2$ which is parallel to that of the magnetic field lines in the neighbourhood of the sun (36). This coincidence in the directions suggests the random gas motions are either strongly influenced by the local magnetic field or that both the gas motion and the field are influenced in the same way by some other perturbation.

The Lindblad-Oort theory also requires that the third axis of the ellipsoid which should point toward the pole of the Milky Way be equal in length to the longer axis in the plane, and the ratio of the two axes which lie in the plane $(\Sigma_1/\Sigma_2) = 1.5$. In our analysis we obtain $\Sigma_1 = 6.7$ KmS^{-1} and $\Sigma_3 = 7.8$ KmS^{-1}, and the ratio $\left(\Sigma_1/\Sigma_2\right) = 1.51$.

The agreement between our observations of these quantities and the predictions of the Lindblad-Oort theory is good, but it is not clear whether it should be expected if the Lindblad-Oort theory were reformulated to take account of the effects of the local magnetic field, so that further theoretical analysis seems desirable.

It is also of interest to compare the velocity ellipsoid elements for the gas with those for B stars given by Nördstrom (49). They are

$$\Sigma_1 = 12{\cdot}4 \text{ km s}^{-1} \qquad l = 266^\circ{\cdot}3 \qquad b = +33^\circ{\cdot}9$$

$$\Sigma_2 = 10{\cdot}7 \text{ km s}^{-1} \qquad l = 170^\circ{\cdot}4 \qquad b = +10^\circ{\cdot}0$$

$$\Sigma_3 = 5{\cdot}1 \text{ km s}^{-1} \qquad l = 246^\circ{\cdot}6 \qquad b = -54^\circ{\cdot}3$$

It should be noted that the velocity dispersion of B stars is appreciably greater than that of neutral hydrogen gas, and for late type stars the dispersion is even greater than that for B stars.

We suggest a similar progression applies for the vertex longitude. The longitude of the vertex for B stars ($l = 266^\circ.3$) is about 27° further from the anticentre than that for the gas.

For the later type stars the vertex direction is $l \approx 200^\circ$. However, the vertex longitude for B stars is not well defined, since the axes Σ_1 and Σ_2 of the velocity ellipsoid are very nearly equal and there seems to be some difficulty in deciding which of these axes corresponds to the vertex. Bearing these uncertainties in mind we suggest, after consideration of the available data for B stars (16), that the vertex direction is towards $l \approx 220^\circ$, midway between that for the gas and that for the later type stars.

We therefore suggest, as an explanation of the observations, that the vertex direction of all classes of stars are found to be towards longitudes greater than $\ell = 180^\circ$ suggested by theory, that these stars were formed from gas with maximum random motions aligned with $\ell = 240^\circ$ and have gradually relaxed towards the direction $\ell = 180^\circ$ required by theory. During this relaxation process themagnitude of the random velocities has increased progressively.

DEPARTURE FROM CIRCULAR MOTION

Although it is clear that the gas motions are predominantly circular in most parts of the Galaxy it has also been noticed that important deviations from perfect circular motion do exist in the over-all velocity field of the Galaxy. Hence an investigation of the departure of the gas motion from the circular motion according to the Oort-Lindblad theory of galactic rotation was undertaken to see if our data could suggest any systematic departure from circular motion.

In the last chapter it has been mentioned that a linear relationship $\overline{V}_{obs} - \alpha \overline{V}_{th} = V$ was considered and that the value of α found for which $\sum V^2$ was a minimum. The constant α indicates the nature of the peculiar velocities $\overline{V}_p$. If $\alpha = 1$, the mean of all values $\overline{V}$ tends to zero. If α deviates from 1 the mean is non-zero and the value $\overline{AZ_o}$ must be corrected to $\alpha \overline{AZ_o}$ to allow for the bias so introduced. Then the residuals $\overline{V}_{obs} - \alpha \overline{V}_{th} = V$ can be used to study the departures from circular motion.

A plot of the residuals V obtained in the analysis of last chapter against the longitude (l) for each latitude (b) seemed to suggest a significant cos 2l variation. A cos 2l variation of the residuals suggests a possibility of the existence of radial motion in our Galaxy. In fact, there is observational evidence both for our own (59, 40) and for external galaxies (11) that radial motions exist in regions with dimensions of a few Kiloparsecs and that the circular and radial motions may not be axisymmetric. Hence an attempt has been made to see if any systematic radial motion could be detected from our data.

Trumpler and Weaver (66c) and Rubin and Burley (60) have derived expressions for the radial velocity of stars with respect to the local standard of rest resulting from the combined effect of galactic rotation and radial motion. The expression for the differential velocity for the solar vicinity is:

$$V_r = r \cos^2 b \left[A \sin 2l + C \cos 2l + D \right] \text{-----} 43$$

where r is the distance of the star to the sun and A is the usual Oort constant and C and D are Oort-like constants.

Since in the stratified layer model $r = Z_o \operatorname{cosec} b$,

$$V_r = Z_o \operatorname{Cosec} b \cos^2 b \left[A \sin 2l + C \cos 2l + D \right] \quad 44$$

In this analysis 168 profiles in the northern intermediate latitudes (15° to 40°) covering 360° in longitude and 119 profiles in the southern intermediate latitudes covering the longitude range 0° to 230° were made use of. The mean velocity of each profile was determined and a least squares solution was made to determine the constants Z_o, C and D assuming the value of 15.0 KmS^{-1} Kpc^{-1} for the Oort constant A. Separate solutions were made for the northern profiles (168), the southern profiles (119) and the combined profiles (287) with the following results:

	No. of Profiles	Z_o Kpc	C KmS^{-1}.	D Kpc^{-1}
Northern Profiles	(168)	0.120	7.2	-2.4
Southern Profiles	(119)	0.095	10.8	8.9
All Profiles	(287)	0.109	8.5	1.8

These results can also be expressed by means of the following expression (66c):

$$V_r = Z_0 \operatorname{Cosec} b \operatorname{Cos}^2 b \left[A_1 \operatorname{Sin} 2(l+h) + D\right] \text{-----} 45$$

where $A_1 = \sqrt{A^2+C^2}$ and $\tan 2h = -\frac{C}{A}$. This means that in the case of a radial motion combined with a rotational motion: (1) the radial velocity formula contains a term independent of the longitude (2) the double sine variation of radial velocity has a different phase; the longitude at which the first term vanishes is not the longitude of the galactic centre ($l = 0°$). Expressing our previous results in this form with a phase shift the three cases yield respectively:

1. Northern latitudes:

$$V_r = 0.120 \operatorname{Cosec} b \operatorname{Cos}^2 b \left[16.7 \operatorname{Sin} 2(l + 12°.9) - 2.4\right] \text{Km}\,\text{s}^{-1}$$

with probable errors for h and D of $\pm 4°.6$ and $\pm 0.6\ \text{Km}\,\text{s}^{-1}$ respectively.

2. Southern latitudes:

$$V_r = 0.095 \operatorname{Cosec} b \operatorname{Cos}^2 b \left[18.5 \operatorname{Sin} 2(l + 17°.8) + 8.9\right] \text{Km}\,\text{s}^{-1}$$

3. All latitudes:

$$V_r = 0.109 \operatorname{Cosec} b \operatorname{Cos}^2 b \left[17.3 \operatorname{Sin} 2(l + 14°.9) + 1.8\right] \text{Km}\,\text{s}^{-1}$$

Discussion:

Analyses similar to the above have been carried out by Henderson (29) for the longitude range 16° to 230° for latitude $|10°|$ and by Grahl et al (25) for latitude $+30°$.

Their results are:

Henderson (1967) : $V_r = 0.076 \operatorname{cosec} b \cos^2 b \left[15 \sin 2(l + 4°.9) - 0.9\right] \text{Km}\,\text{s}^{-1}$

Grahl et al (1968): $V_r = 0.230 \operatorname{cosec} b \cos^2 b \left[15 \sin 2(l + 18°.5) - 6.7\right] \text{Km}\,\text{s}^{-1}$

Equation 43 was developed for the case where the gas motion in addition to the normally assumed circular velocity, has a radial component. A formal interpretation on this basis would suggest a radial component of motion towards the galactic centre of 34 $\text{Km}\,\text{s}^{-1}$

from Henderson's data, 113 KmS^{-1} from the data of Grahl et al, and 97 KmS^{-1} from our data. This interpretation would lead one to expect a velocity difference of about 130 KmS^{-1} between the northern and southern rotation curves of the Galaxy, whereas the observed difference is certainly less than 20 KmS^{-1}. In fact, if we assume the average velocity difference is 10 KmS^{-1} the calculated phase shift h in equation 45 is $<3^{\circ}$, whereas we have determined a value for h of $13^{\circ} \pm 4.6^{\circ}$.

We therefore conclude that the phase shift and departures from circular motion observed are not a result of large scale organized motion in the Galaxy, but a local effect. Since similar analyses for O and B stars (60) show much smaller departures, we look for an explanation in terms of forces which affect the gas but not the stars. An obvious candidate is the local magnetic field, and we would view the phase shift as a shearing effect produced by the local magnetic field.

SUMMARY OF RESULTS AND CONCLUSIONS

Neutral hydrogen line profiles obtained at intermediate galactic latitudes have been used to i) determine the kinetic temperature of nearby gas; ii) determine the solar motion with respect to this gas; iii) derive the velocity ellipsoid describing the random motions of the gas; and iv) study departures of the gas velocities from circular motion.

i) The kinetic temperature of hydrogen obtained on the assumption of horizontal stratification in density is 120° K

ii) The elements of solar motion relative to neutral hydrogen with their probable errors are :

$S_{\odot} = 21{\cdot}1 \pm 1{\cdot}3$ Km S^{-1}, $L_{\odot} = 49^{\circ}{\cdot}2 \pm 8^{\circ}{\cdot}9$, $B_{\odot} = +24^{\circ}{\cdot}7 \pm 13^{\circ}{\cdot}7$,
$K = -0{\cdot}8 \pm 0{\cdot}7$ Km S^{-1}.

iii) The axes of the velocity ellipsoid describing the distribution of random motions of the gas and their directions are:

$\Sigma_1 = 6.7$ KmS^{-1}	$l = 239^{\circ}.2$	$b = +35^{\circ}.3$
$\Sigma_2 = 4.5$ KmS^{-1}	$l = 160^{\circ}.3$	$b = -14^{\circ}.9$
$\Sigma_3 = 7.8$ KmS^{-1}	$l = 269^{\circ}.0$	$b = -49^{\circ}.8$

$$\text{Mean dispersion} = (\bar{\Sigma}) = \sqrt{1/3\left[(\Sigma_1)^2 + (\Sigma_2)^2 + (\Sigma_3)^2\right.}$$
$$= 6{\cdot}5 \text{ Km } S^{-1}$$

and:

iv) The observed mean velocities of the gas at intermediate galactic latitudes may be represented by the following expression:

$$\overline{V}_{obs} = 0{\cdot}120 \operatorname{Cosec} b \operatorname{Cos}^2 b \left[16{\cdot}7 \operatorname{Sin} 2(l + 12^{\circ}{\cdot}9) - 2{\cdot}4\right] \text{Km } S^{-1}$$

On the basis of the above results the following conclusions are drawn:

i) That in the vicinity of the sun there is no appreciable differential motion between the neutral hydrogen and the stars;

iia) That the vertex direction of the velocity ellipsoid is found to be closely aligned with the local magnetic field, supporting the view that the random motion is influenced by the field;

iib) That the vertex directions of all classes of stars are found to be towards longitudes greater than $\ell = 180^{\circ}$; that these stars were formed from gas with maximum random motions aligned with $\ell = 240^{\circ}$ and have gradually relaxed towards $\ell = 180^{\circ}$, and that during the relaxation process the magnitude of the random velocities has increased progressively and

iii) That the phase shift and departures from circular motion observed are not a result of large scale organized motion in the Galaxy, but a local effect caused probably by the local magnetic field.

BIBLIOGRAPHY

1. Adams, W.S. Ap.J., 109, 354 (1940)

2. Adler, R., Hrbek, G., and Wade, G. Proc. I.R.E., 47, 1713 (1959)

3. Barrett, A.H., Proc. I.R.E., 46, 250 (1958)

4. Beehler, R. et al Proc. I.E.E.E., 54, 301 (1966)

5. Bethe, H.A., Hdb.d.Phys., (Berlin: Springer Verlag) 24/1, 385 (1933)

6. Bethe, H.A., and Salpeter, E.E., Hdb.d.Phys., (Berlin: Springer Verlag) 35, 193 (1957)

7. Blaauw, A., Gum, C.S., Pawsey, J.L., and Westerhout, G. Mon. Not. Roy. Astr. Soc., 121, 123 (1960)

8. Bok, B.J., Lawrence, R.S., and Menon, T.K., Pub. A.S.P., 67, 108 (1955)

9. Bolton, J.G., and Wild, J.P., Ap. J., 125, 296 (1957)

10. Braes, L.L.E., B.A.N., 17, 132 (1963)

11. Burbidge, E.M., Burbidge, G.R., and Prendergast, K.H., Ap.J., 134, 232 (1961)

12. Chandrasekhar, S., Principles of Stellar Dynamics (Dover Publications, Inc. New York), 3 (1960)

13. Clark, B.G., Observations of Owens Valley Radio Observatory, California Institute of Technology no. 6, (1965)

14. Davies, R.D., Mon. Not. Roy. Astr. Soc., 116, 443 (1956)

15. Davies, R.D., Mon. Not. Roy. Astr. Soc., 120, 483 (1960)

16. Delhaye, J., Stars and Stellar Systems, (University of Chicago Press) V, 61 (1965)

17. Donn, B., A.J., 60, 237 (1955)

18. Donn, B., Rev. Mod. Phys., 30, 940 (IAU Symp. No. 8) (1958)

19. Edmondson, F.K., Trans. I.A.U. II B, 393 (1962)

20. Elvius, T., Stars and Stellar Systems (University of Chicago Press) V, 41 (1965)

21. Erickson, W.C., and Helfer, H.L., A.J., 65, 1 (1960)

22. Erickson, W.C., Helfer, H.L., and Tatel, H.E., Paris Symposium on Radio Astronomy (IAU Symp. No. 9) 390 (1959)

23 (a) Ewen, H.I., and Purcell, E.M., Phys. Rev., 83, 881 (1951)

(b) Ewen, H.I. and Purcell, E.M., Nature, 168, 356 (1951)

24. Field, G.B., Proc. I.R.E., 46, 240 (1958)

25. Grahl, B.H., Hachenberg, O., and Mebold, U., Beitrage Zur Radio Astronomie (Max Planck Institute) Band 1, Heft 1. (1968)

26. Heiles, C.H., Ap. J. Suppl. No 136 (1967)

27. Heiles, C.H., Ap. J., 151, 919 (1968)

28. Helfer, H.L., and Tatel, H.E., Ap. J., 129, 565 (1959)

29. Henderson, A.P., Ph.D. Thesis, University of Maryland (1967)

30. Herrick, S., Lick Observatory Bulletin No. 470 (1935)

31. Hiltner, W.A., Science, 109, 165 (1949)

32. Hiltner, W.A., Ap. J., 114, 241 (1951)

33. Hogg, H.S., Hdb. d. Phys., (Berlin: Springer: Verlag) 53, 129 (1959)

34. Van de Hulst, H.C., Ned. Tijdschr. Natuurk, 11, 210 (1945)

35. Van de Hulst, H.C., Muller, C.A., and Oort, J.H., B.A.N. 12, 117 (1954)

36. Van de Hulst, H.C., Ann. Rev. Astr. Astrophys., 5, 179 (1967)

37. Jansky, K.G., Proc. I.R.E., 20, 1920 (1932)

38. Jansky, K.G., Nature, 132, 66 (1933)

39. Kahn, F.D., Gas Dynamics of Cosmic Clouds (North Holland Publishing Co., N.Y.), 60 (1955)

40. Kerr, F.J., Mon. Not. Roy. Astr. Soc., 123, 327 (1962)

41. Lilley, A.E., Ap. J., 121, 559 (1955)

42. Locke, J.L., Galt, J.A., and Costain, C.H., Publications of Dominion Observatory, 25, 77 (1965)

43. McGee, R.X., and Murray, J.D., Aus. J. Phy., 14, 260 (1961)

44. McGee, R.X., Murray, J.D., and Pawsey, J.L., Nature, 189, 957 (1961)

45. Morgan, W.W., Sharpless, S., and Osterbrock, D.E., A.J., 57, 3 (1952)

46. Morgan, W.W., Whitford, A.E., and Code, A.D., Ap. J., 118, 318 (1953)

47. Muller, C.A., and Oort, J.H., Nature, 168, 358 (1951)

48. Munch, G., Ap. J., 125, 42 (1957)

49. Nordstrom, H., Meddel. Lund., Ser. II, No. 79 (1936)

50. Oort, J.H., B.A.N., 6, 249 (1932)

51. Oort, J.H., B.A.N., 15, 45 (1960)

52. Oort, J.H., Kerr, F.J., and Westerhout, G., Mon. Not. Roy. Astr. Soc., 118, 379 (1958)

53. Pawsey, J.L., Nature, 168, 358 (1951)

54. Purcell, E.M., and Field, G.B., Ap. J., 124, 542 (1956)

55. Radhakrishnan, V., Pub. A.S.P., 72, 296 (1960)

56. Reber, G., Ap. J., 91, 621 (1940)

57. Reber, G., Proc. I.R.E., 30, 367 (1942)

58. Riegel, K.W., A.J., 73, S199 (1968)

59. Rougoor, G.W., and Oort, J.H., Proc. Natl. Acad. Sci., U.S., 46 (1960)

60. Rubin, Vera C., and Burley, Jaylee, A.J., 69, 80 (1964)

61. Shklovsky, I.S., Astr. Zhur. SSSR. 26, 10 (1949)

62. Shuter, W.L.H., and Verschuur, G.L., Mon. Not. Roy. Astr. Soc., 127, 387 (1964)

63. Smart, W.M., Stellar Dynamics (Cambridge University Press), 397 (1938)

64. Smith, F.G., Nature 218, 325 (1968)

65. Takakubo, K., Sendai Astronomiaj Raportej Nos. 86 and 87.

66. Trumpler, R.J., and Weaver, H.F., Statistical Astronomy (Dover Publications, Inc., New York) a)566 b)299 & 66 c)581 (1962)

67. Venugopal, V.R., and Shuter, W.L.H., A.J., 72, 534 (1967)

68. Verschuur, G.L., Phy. Rev. Letters, 21, 775 (1968)

69. Weaver, H.W., The Galaxy and the Magellanic Clouds (IAU Symp. No. 20) 92 (1964)

70. Weinreb, S., Barrett, A.H., Meeks, M.L. and Henry, J.C., Nature, 200, 829 (1963)

71. Westerhout, G., B.A.N., 13, 201 (1957)

72. Wild, J.P., Ap. J., 115, 206 (1952)

73. Woltjer, L. Stars and Stellar Systems (University of Chicago Press) V, 571 (1965)

Table I. THE CLASSIFICATION OF STELLAR POPULATIONS AT THE VATICAN CONFERENCE 1957.

(Ref: Blaauw, A., Stars and Stellar Systems, University of Chicago Press, V, 444, 1965)

(1) $\langle|z|\rangle$ Mean distance from plane

(2) $\langle|\dot{Z}|\rangle$ Mean velocity component perpendicular to the galactic plane.

(3) $Z_{h.e.}$ Interstellar abundance of elements heavier than Helium.

TABLE I

	Population II		Disk Population	Population I	
	Halo Pop. II	Intermediate Pop. II		Older Pop. I	Extreme Pop. I
	Subdwarfs Globular clusters RR Lyrae stars with periods longer than 0.4 days	High-velocity stars with z-velocities > 30 km/sec Long period variables with periods <250 days and spectral types earlier than M5e	Stars of galactic nucleus Planetary nebulae Novae RR Lyrae stars with periods <0.4 days Weak-line stars	A-type stars Strong line stars Me dwarfs	Gas Young stars associated with the present spiral structure Supergiants Cepheids T Tauri stars Galactic clusters of Trumpler's class I
$\langle \lvert z \rvert \rangle^{(1)}$ (parsecs)	2000	700	400	160	120
$\langle \lvert Z \rvert \rangle^{(2)}$ ($Km\ S^{-1}$)	75	25	17	10	8
Axial ratio of spheroidal distribution	2	5	25?	?	100
Concentration toward center	Strong	Strong	Strong?	Little	Little
Distribution	Smooth	Smooth	Smooth?	Patchy spiral arms	Extremely Patchy spiral arms
$Z_{h.e.}^{(3)}$	0.003	0.01	0.02	0.03	0.04
Age (10^9 years)	6	6.0 to 5.0	1.5 to 5.0	0.1 to 1.5	< 0.1
Total mass (10^9 ⊙)	16	47		5	2

Figure 1. STRUCTURE OF THE GALAXY

(Source: Atlas of the Universe, Thomas Nelson & Sons Ltd. 1961)

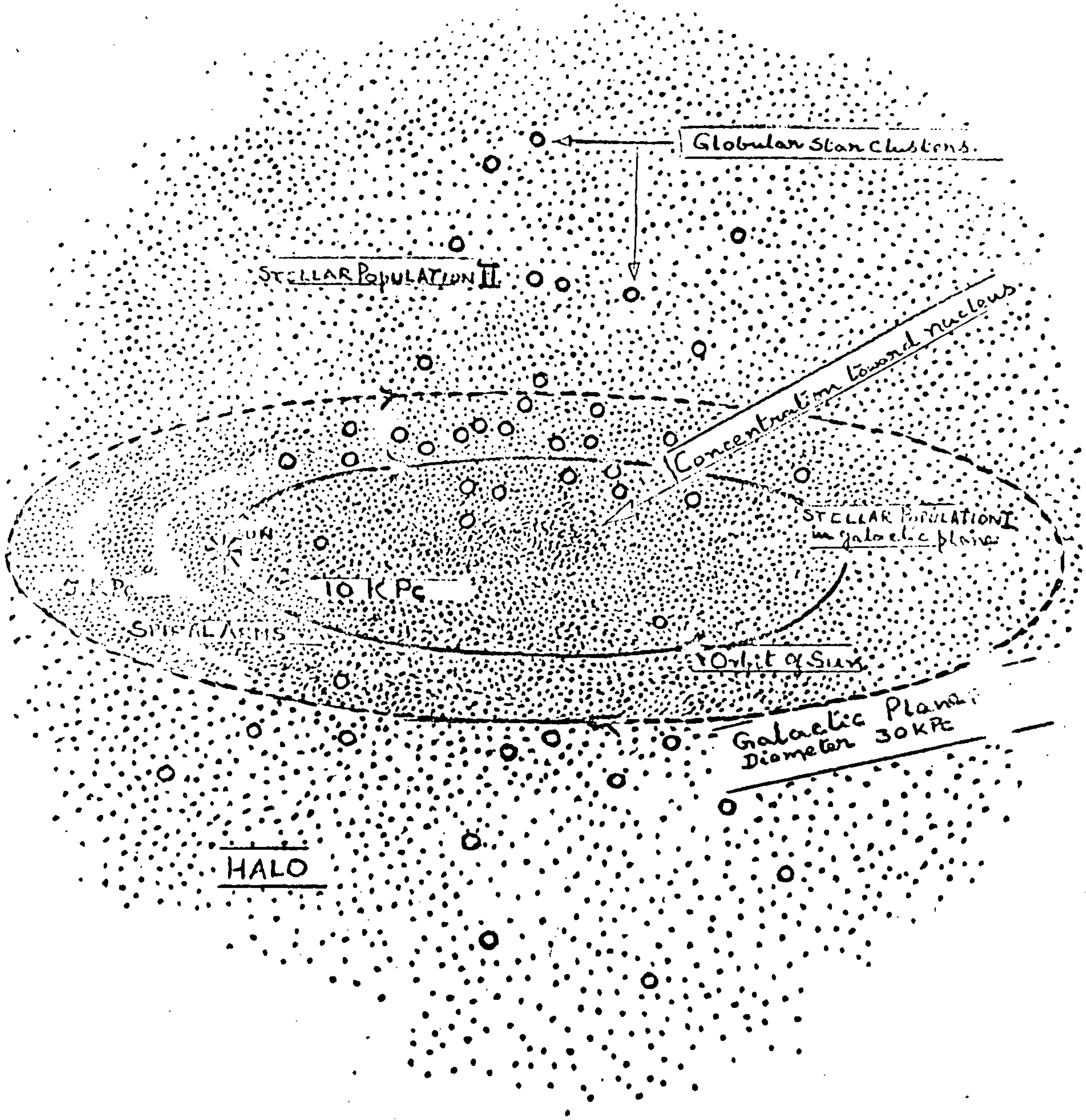

Globular star clusters.
STELLAR POPULATION II
Concentration toward nucleus
STELLAR POPULATION I in galactic plane
SUN
10 KPc
SPIRAL ARMS
Orbit of Sun
Galactic Plane Diameter 30 KPc
HALO

FIG. 1.

Figure 2. MERIDIAN SECTION OF THE GALAXY THROUGH THE SUN
(Ref: Blaauw,A., Stars and Stellar Systems,
University of Chicago Press,V, 440, 1965)

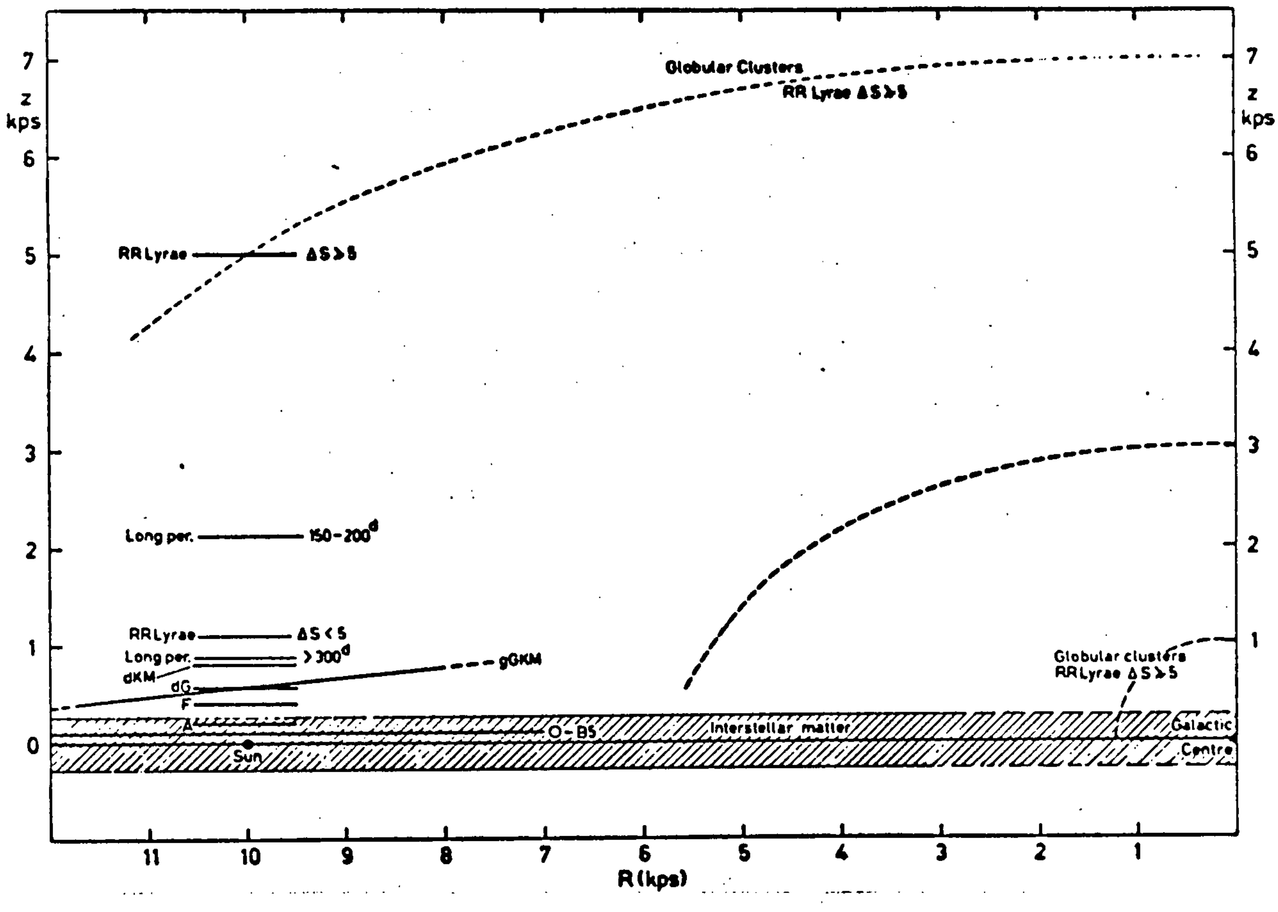

Globular Clusters
RR Lyrae ΔS≥5
RR Lyrae ΔS≥5
Long per. 150-200^d
RR Lyrae ΔS<5
Long per. >300^d
dKM
dG
F
A
gGKM
O-B5
Interstellar matter
Sun
Globular clusters
RR Lyrae ΔS≥5
Galactic
Centre
z
kps
R (kps)

FIG. 2.

Figure 3. AN IDEALIZED PICTURE OF THE SPIRAL PATTERN OF THE GALAXY.
Shaded areas outline the arms formed by the O-Associations
Longitudes refer to the New Galactic Coordinate System

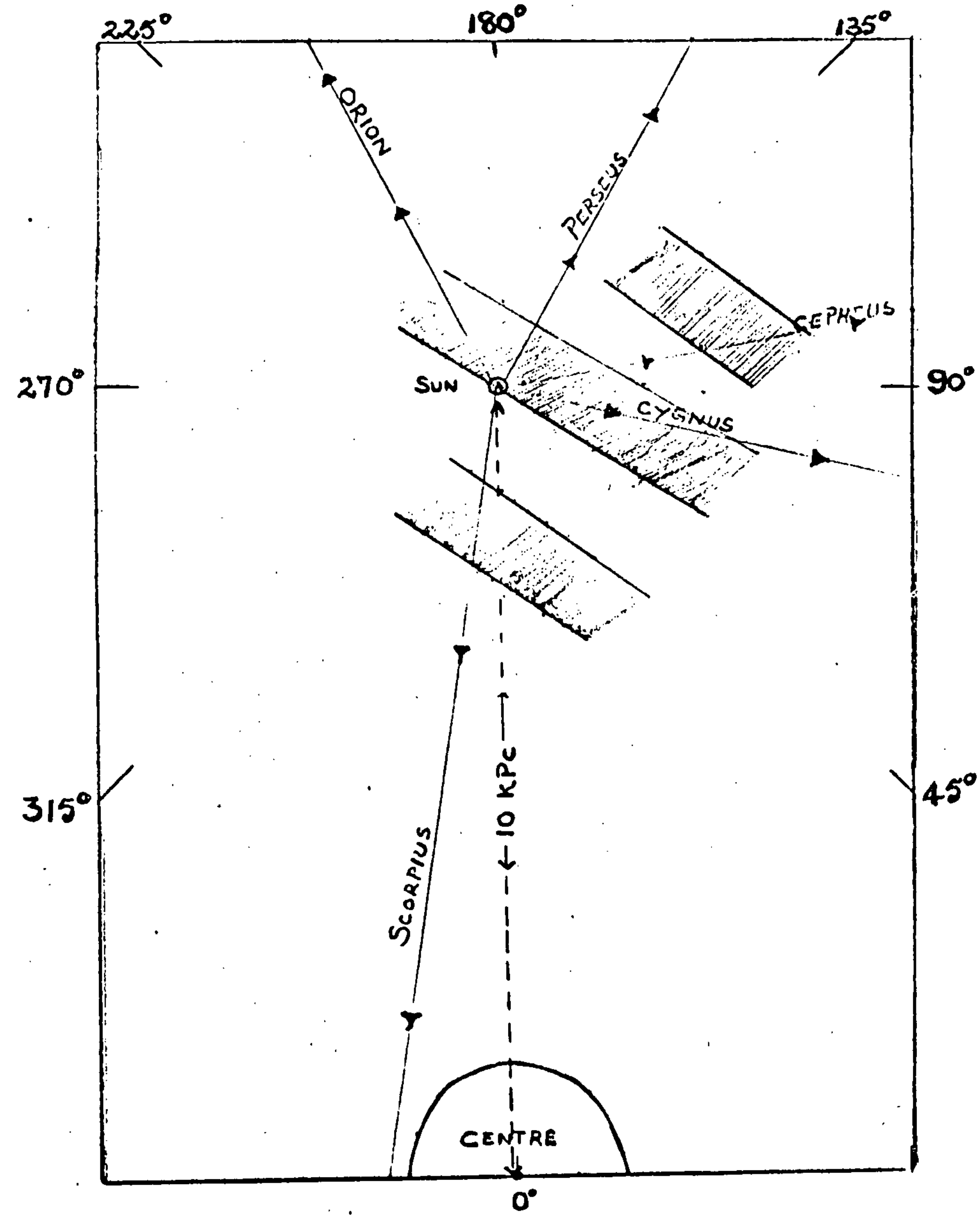

225°
180°
135°
ORION
PERSEUS
CEPHEUS
270°
SUN
CYGNUS
90°
10 KPC
315°
SCORPIUS
45°
CENTRE
0°

FIG. 3.

Figure 4. STRATIFIED MODEL REPRESENTATION OF THE GALAXY IN THE SOLAR NEIGHBOURHOOD.

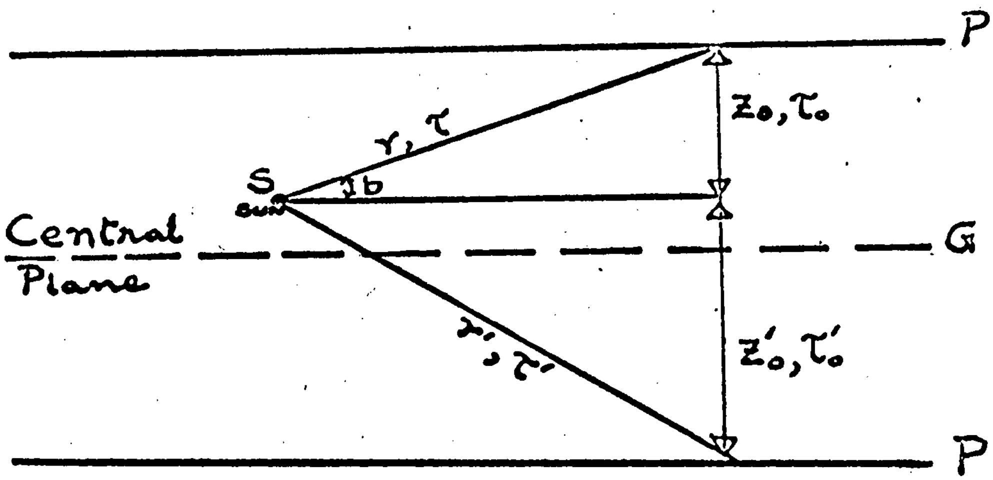

FIG. 4.

Figure 5. PLOT OF OPTICAL DEPTH (τ) AGAINST COSEC b FOR NORTHERN GALACTIC HEMISPHERE.

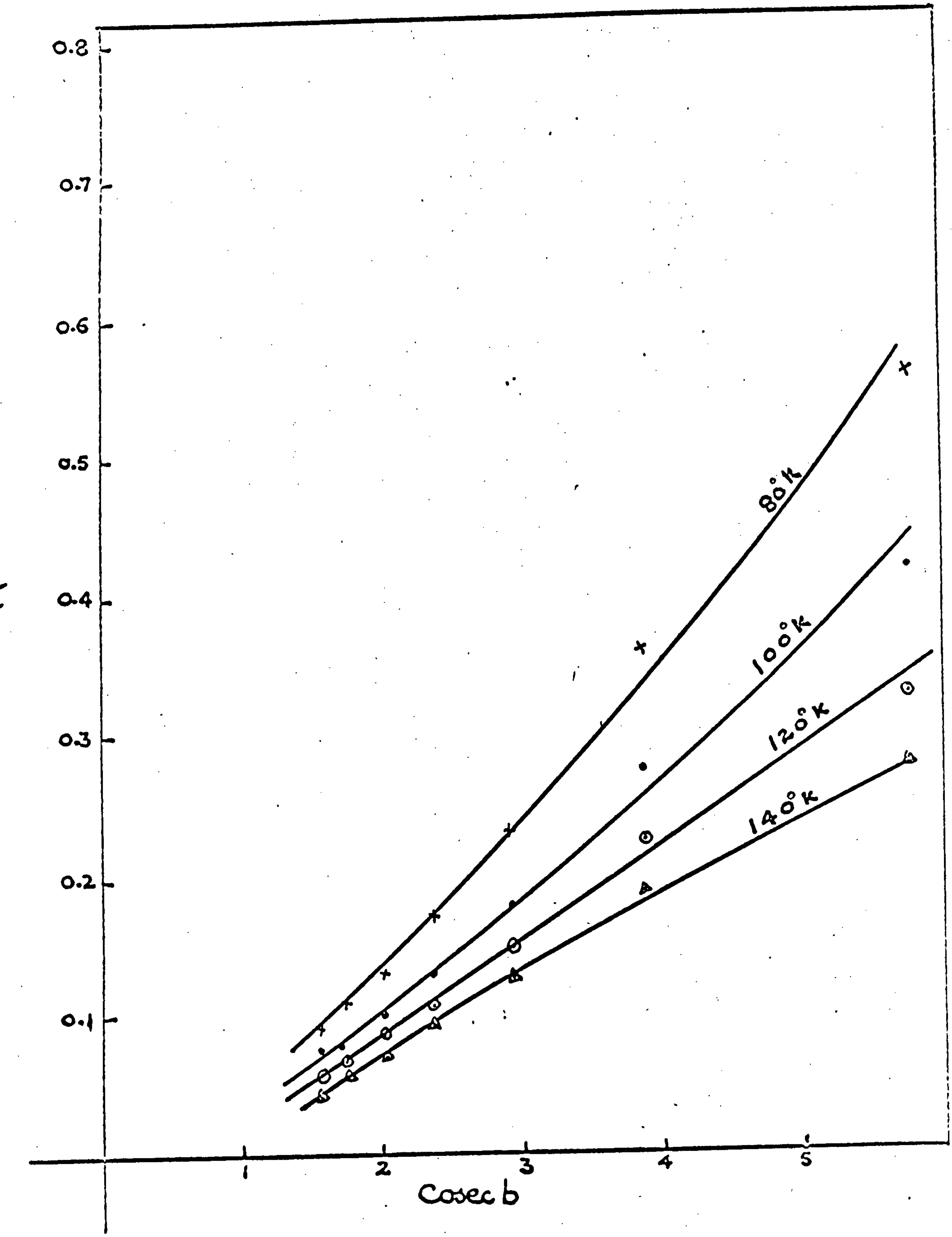

FIG. 5.

Figure 6. PLOT OF OPTICAL DEPTH (τ) AGAINST COSEC b FOR SOUTHERN GALACTIC HEMISPHERE.

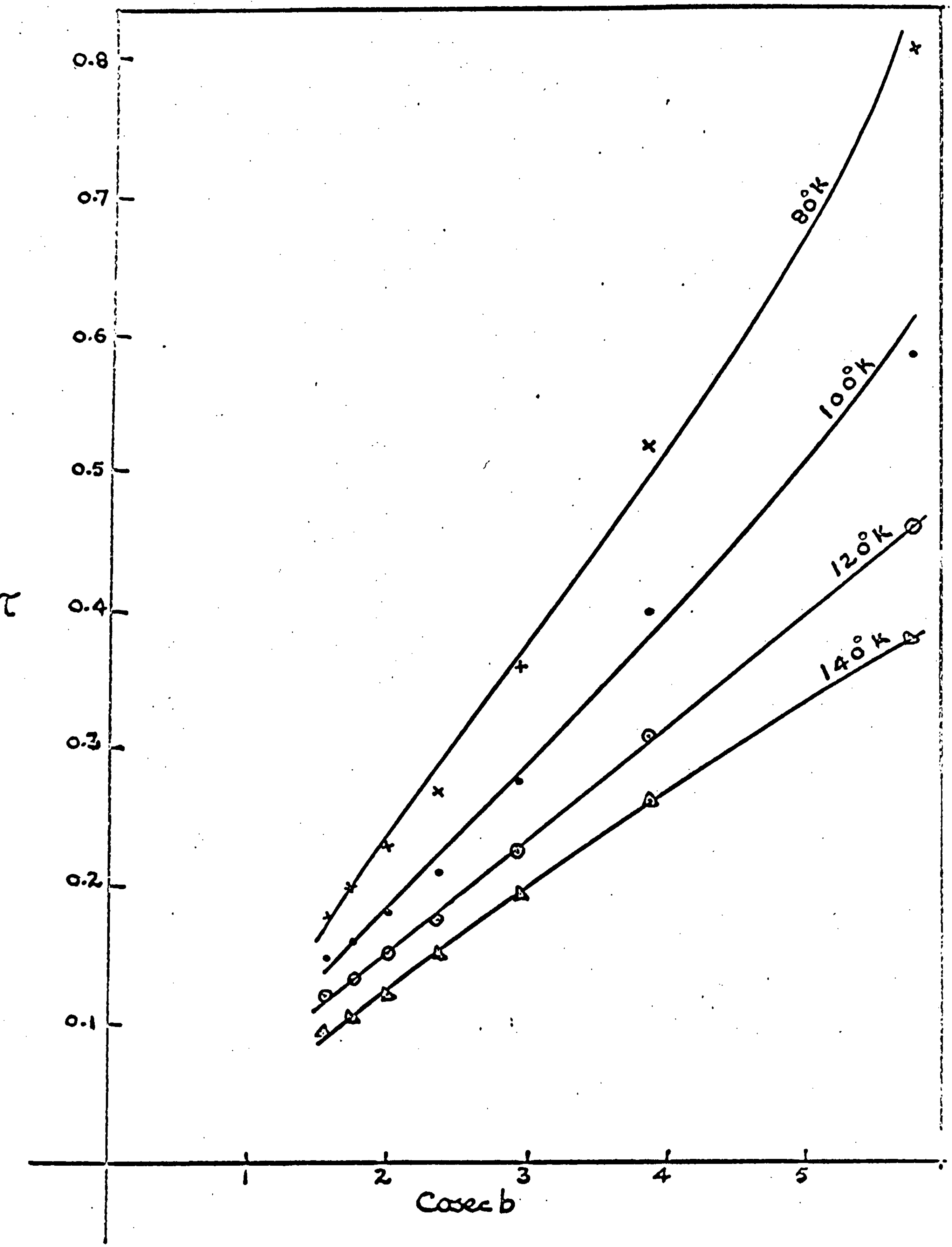

FIG. 6.

Figure 7. TYPICAL 21-cm. LINE PROFILES.

a) In the direction of the Galactic centre.

b) At $b = 0^{\circ}$, $\pm 15^{\circ}$ & $\pm 20^{\circ}$

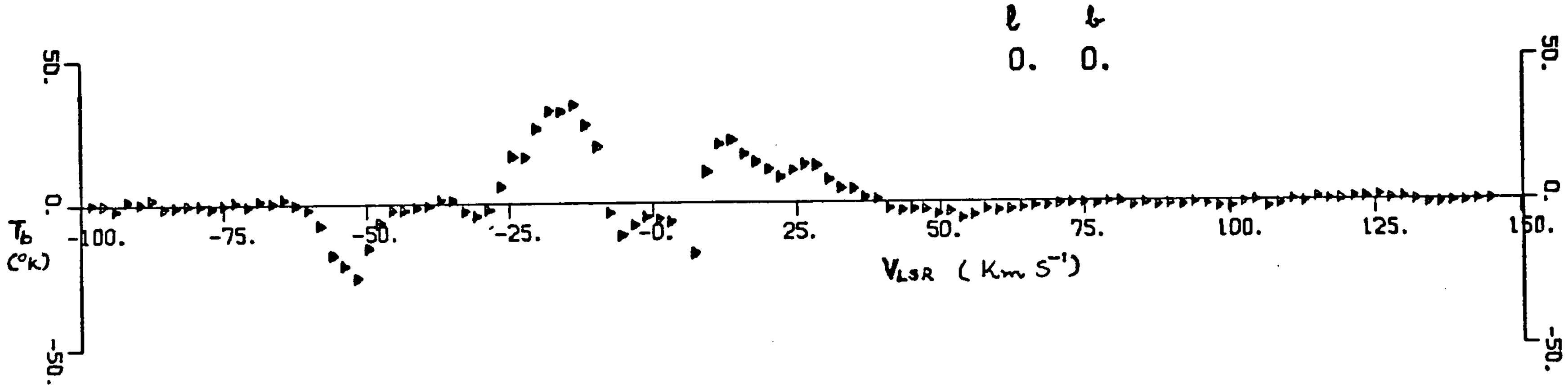

l b
0. 0.
50.
0.
-50.
Tb (°K)
-100.
-75.
-50.
-25.
-0.
25.
50.
75.
100.
125.
150.
VLSR (Km S-1)

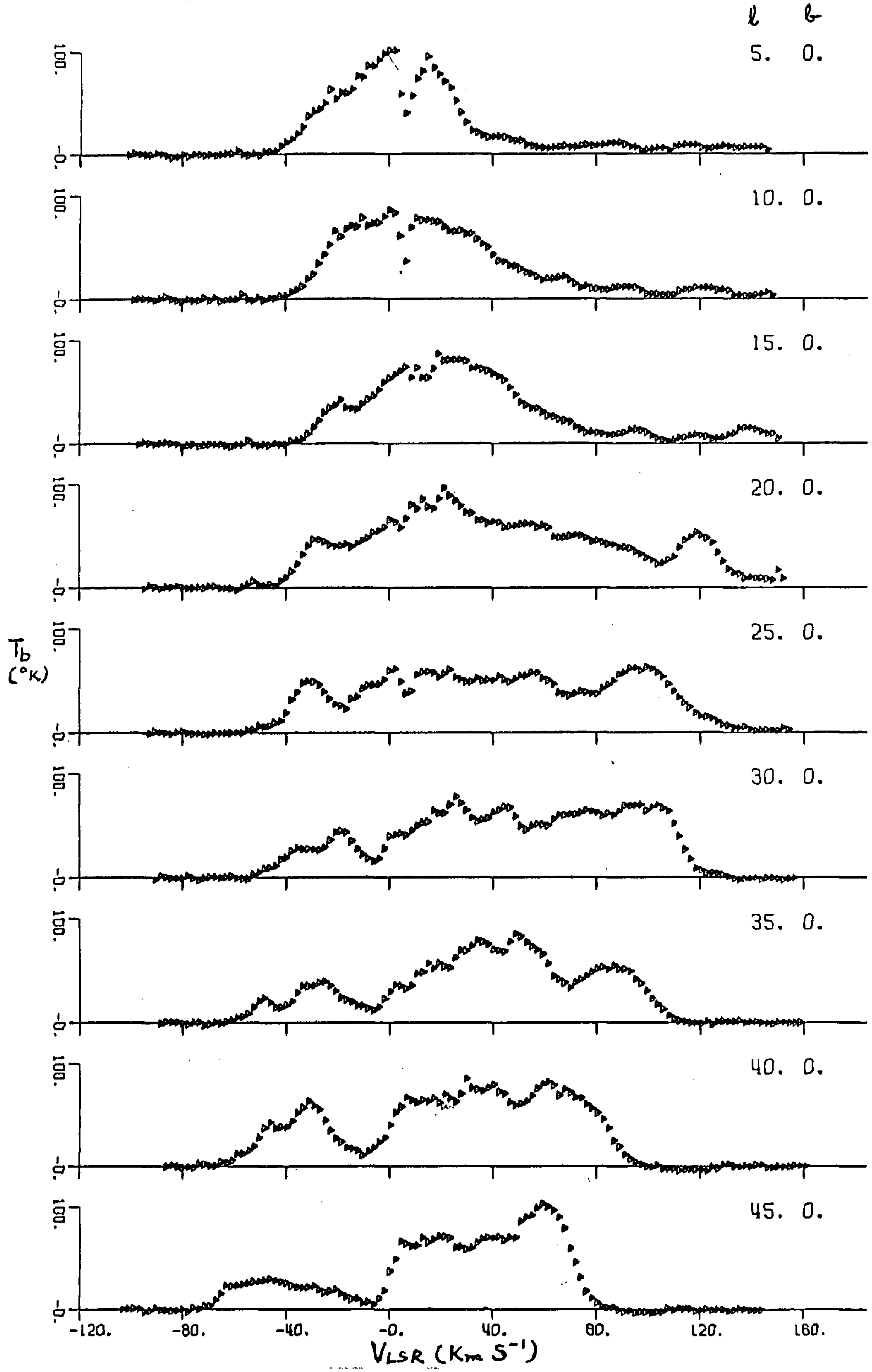

l b
5. 0.
10. 0.
15. 0.
20. 0.
25. 0.
30. 0.
35. 0.
40. 0.
45. 0.
100.
0.
Tb (°K)
-120.
-80.
-40.
-0.
40.
80.
120.
160.
VLSR (Km S-1)

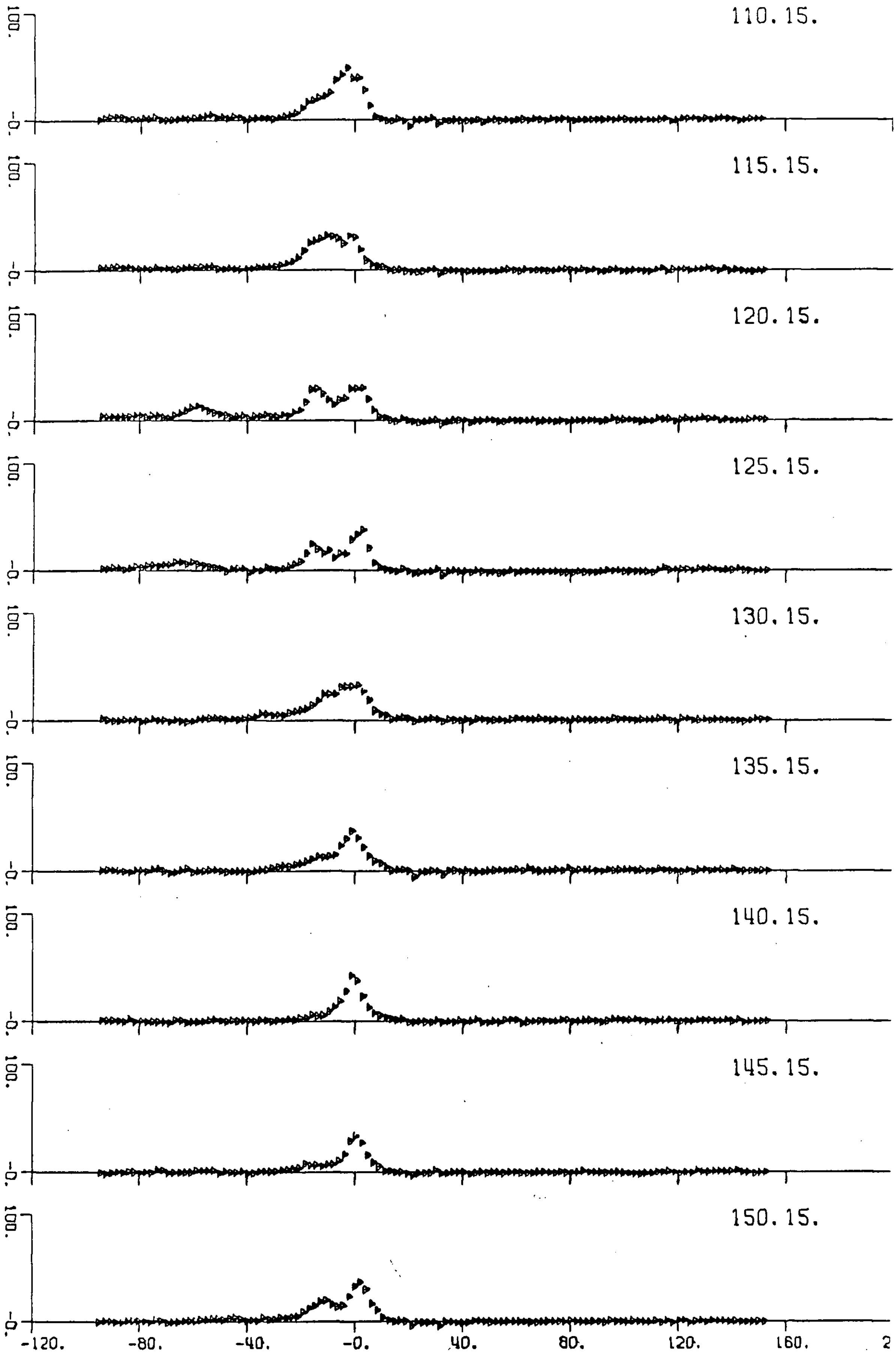
110.15.
115.15.
120.15.
125.15.
130.15.
135.15.
140.15.
145.15.
150.15.
100.
-0.
-120.
-80.
-40.
-0.
40.
80.
120.
160.
2

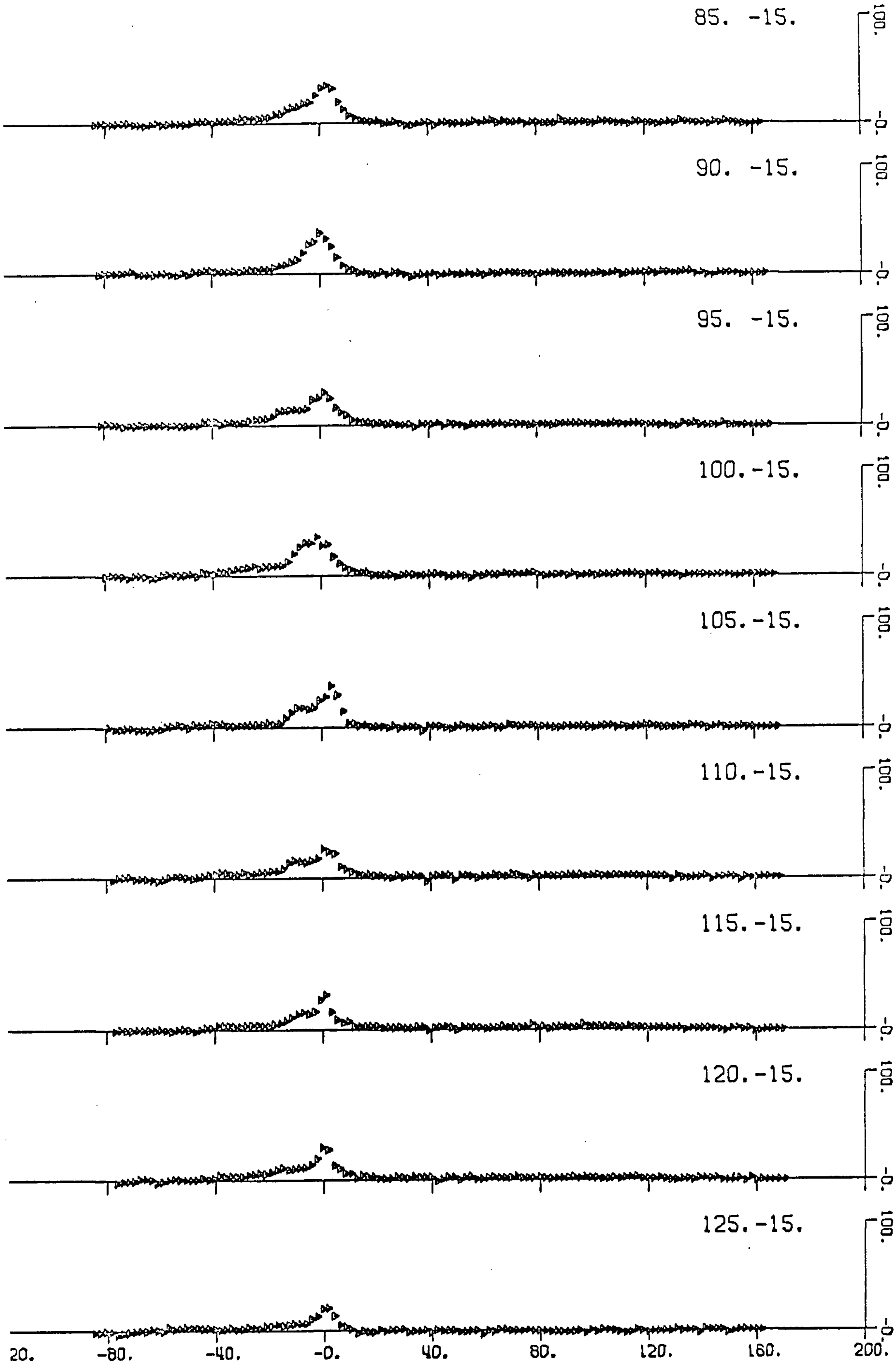

85. -15.
90. -15.
95. -15.
100.-15.
105.-15.
110.-15.
115.-15.
120.-15.
125.-15.
100.
-0.
20.
-80.
-40.
-0.
40.
80.
120.
160.
200.

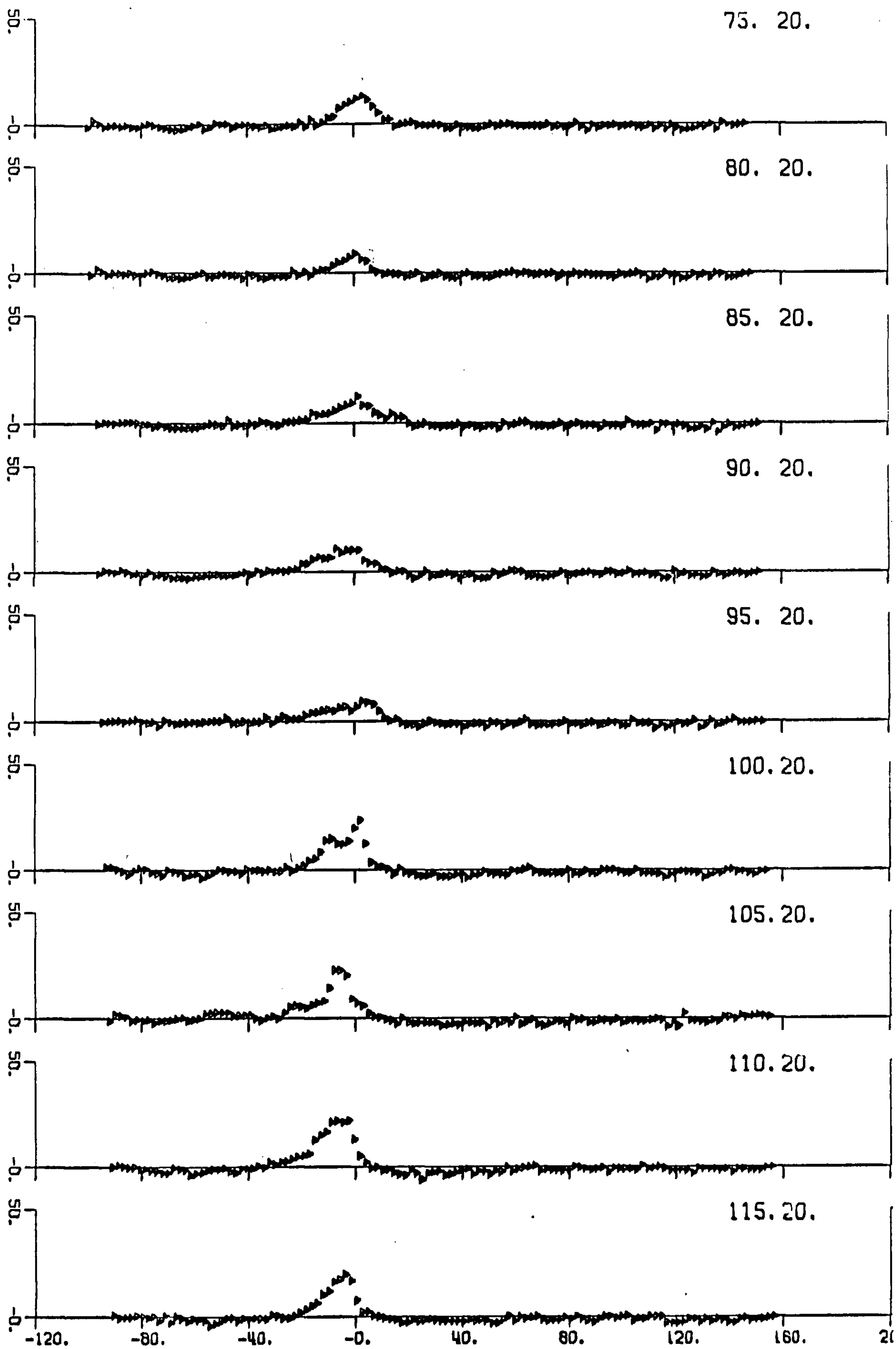
75. 20.
80. 20.
85. 20.
90. 20.
95. 20.
100. 20.
105. 20.
110. 20.
115. 20.
50.
0.
-120.
-80.
-40.
-0.
40.
80.
120.
160.

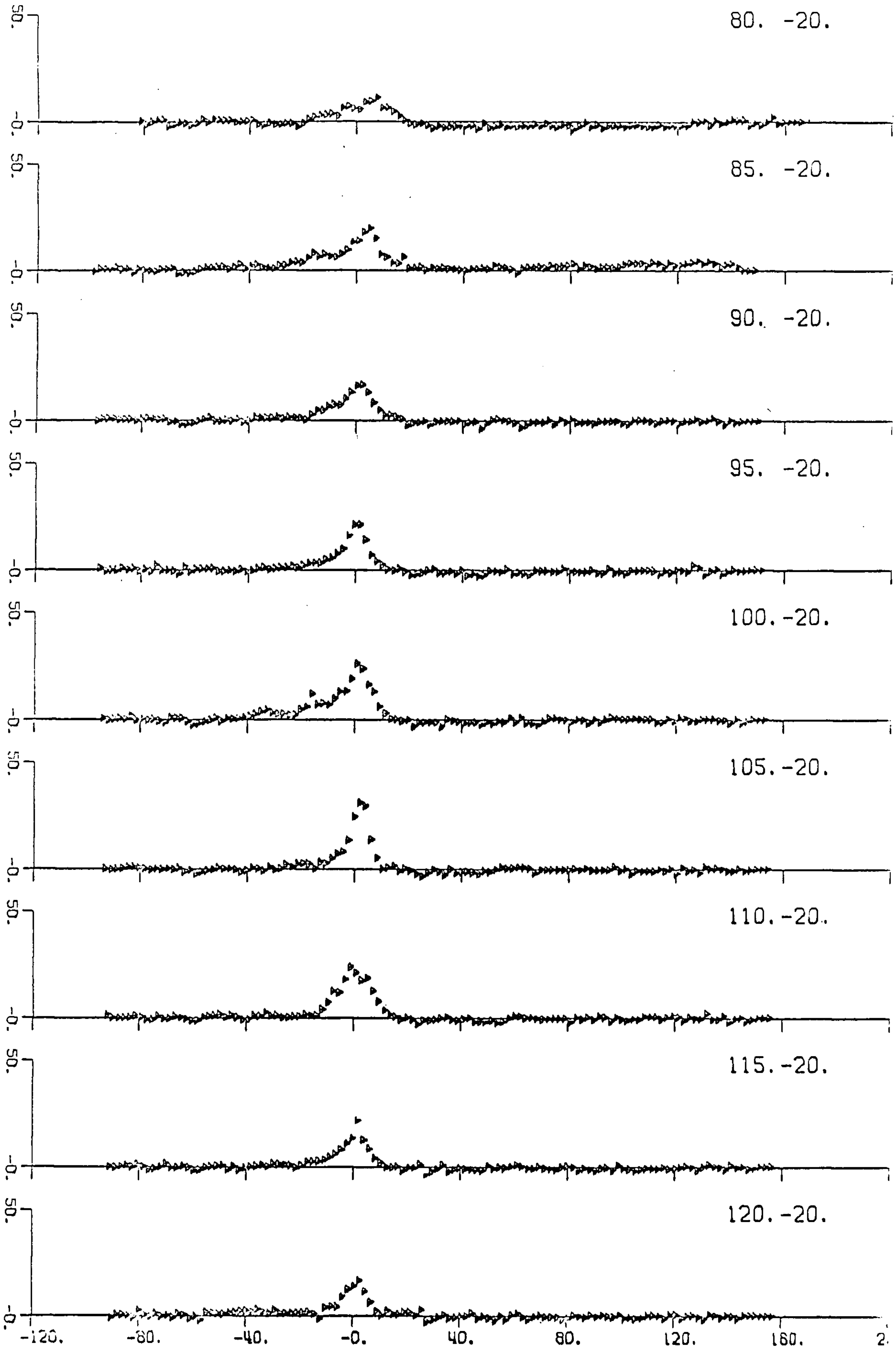

80. -20.
85. -20.
90. -20.
95. -20.
100. -20.
105. -20.
110. -20.
115. -20.
120. -20.
50.
-0.
-120.
-80.
-40.
-0.
40.
80.
120.
160.